

# Chapter 8

## The Behavior of Halogens During Subduction-Zone Processes

Jaime D. Barnes, Craig E. Manning, Marco Scambelluri  
and Jane Selverstone

**Abstract** Halogens (Cl, F, I, Br) are enriched in surface reservoirs compared to the mantle. The subduction of these reservoirs in the form of sedimentary pore fluids, sediments, altered oceanic crust, and serpentinized mantle lithosphere returns halogens to the mantle and to regions of arc magma genesis. Pore fluids are particularly enriched in I, yet shallow pore fluid loss in subduction zones due to compaction, as indicated by  $^{129}\text{I}/\text{I}$  ratios, makes pore fluids a negligible halogen source at depths  $>\sim 5$  km. Sediments can host large quantities of halogens, particularly I. However, serpentinites  $\pm$  altered oceanic crust subduct the largest amount of halogens to depths of magma genesis. Due to their hydrophilic nature, halogens are lost to aqueous slab-derived fluids during prograde metamorphic reactions. The addition of halogens, particularly Cl, increases the ability of subduction-zone fluids to transport metals and trace elements. The amount of Cl in solution is a function of the P-T conditions of the subduction zone, such that higher temperatures at a given depth and lower pressures at a given temperature favor ion pair formation ( $\text{NaCl}_{\text{aq}}$ ,  $\text{KCl}_{\text{aq}}$ ). Therefore, ion pairing will be more important in subduction zones with warmer geotherms, such as Cascadia, compared to those with cooler geotherms, such as Alaska. High halogen concentrations in melt inclusions and volcanic gas emissions from the arc front support the efficiency of fluid loss and transport from the slab to the region of magma genesis. Despite this high efficiency, mass balance calculations and halogen concentrations in back-arc

---

J.D. Barnes (✉)

Department of Geological Sciences, University of Texas, Austin, TX 78712, USA  
e-mail: jdbarnes@jsg.utexas.edu

C.E. Manning

Department of Earth, Planetary and Space Sciences, University of California,  
Los Angeles, CA 90095-1567, USA

M. Scambelluri

Dipartimento di Scienze Della Terra, Ambiente e Vita DISTAV- Università di Genova,  
Corso Europa 26, 16132 Genoa, Italy

J. Selverstone

Department of Earth and Planetary Sciences, University of New Mexico,  
Albuquerque, NM 87131-0001, USA

© Springer International Publishing AG 2018

D.E. Harlov and L. Aranovich (eds.), *The Role of Halogens in Terrestrial and Extraterrestrial Geochemical Processes*, Springer Geochemistry,  
[https://doi.org/10.1007/978-3-319-61667-4\\_8](https://doi.org/10.1007/978-3-319-61667-4_8)

basalts and ocean island basalts show that more halogens are subducted than returned to the Earth's surface through volcanic arc fronts, implying transport of halogens into the upper mantle. Chlorine is the halogen most efficiently recycled to the surface, and F the least. Shallow loss of I and Br, through fore-arc fluids that are not accounted for in the mass balance calculation, likely explain the imbalance in these cycles.

## 8.1 Introduction

Halogens (F, Cl, Br, and I) are highly mobile in fluids, making them effective tracers of fluid sources within subduction zones. Despite their incompatibility, the relatively small ionic radii of Cl and F permit them to be incorporated into hydrous minerals (e.g., apatite, amphibole, serpentine, micas) in moderate amounts, primarily by exchange for  $\text{OH}^-$ . In contrast, the large ionic radii of Br and I make them highly incompatible. Serpentine is the notable exception among hydrous minerals because of its ability to incorporate up to 45  $\mu\text{g/g}$  I in its structure (Kendrick et al. 2013). The breakdown of different halogen hosts (e.g., amphibole in altered oceanic crust or serpentine in hydrated mantle peridotite) along a subduction zone P-T gradient can be used to trace fluid sources based on diagnostic halogen ratios (F/Cl, I/Cl, Br/Cl) (Fig. 8.1), stable Cl isotope compositions, and  $^{36}\text{Cl}/\text{Cl}$  and  $^{129}\text{I}/\text{I}$  ratios of various reservoirs.<sup>1</sup>

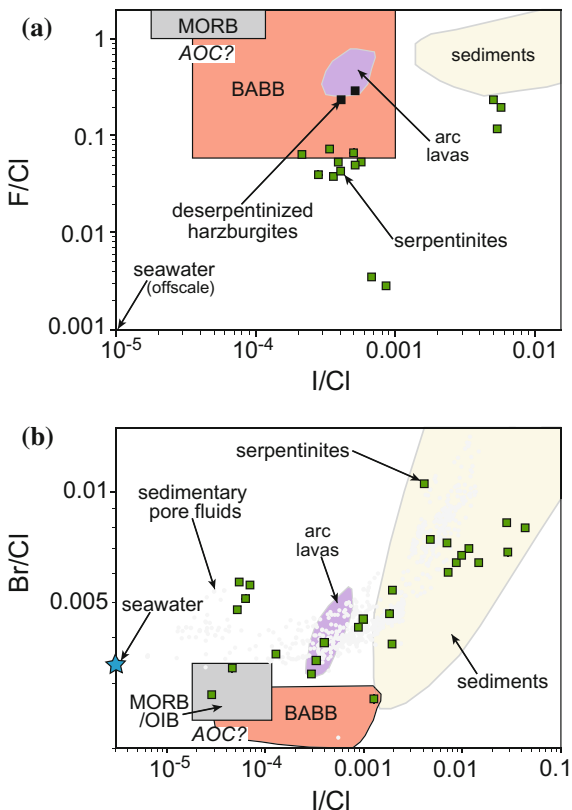
The transport of halogens from the subducting slab to the overlying mantle wedge likely occurs primarily via dissolution in an  $\text{H}_2\text{O}$ -rich fluid produced from the dehydrating slab (e.g., Manning 2004). The addition of halogens, particularly Cl, to subduction-zone fluids changes the physical properties and solute structure compared to pure  $\text{H}_2\text{O}$  (Mantegazzi et al. 2013; Sakuma and Ichiki 2015). For example, saline solutions will suppress the onset of slab melting and cause dehydration reactions to proceed at shallower depths compared to pure  $\text{H}_2\text{O}$  or  $\text{H}_2\text{O}$ - $\text{CO}_2$  fluids (e.g., Aranovich et al. 2013). Additionally, Cl and F complex with metals, suggesting that halogen-rich subduction fluids may be critical in the transport of metals within subduction zones (Keppler 1996, 2017).

The enrichment of halogens in arc magmas has long been cited as evidence for subduction of surface reservoirs. For example, melt inclusions from basaltic arc

---

<sup>1</sup>Halogens can also be transported via melt and "slab diapirs" (Behn et al. 2011; Gerya et al. 2003). For example, F may be more mobilized in melt compared to fluid (Straub and Layne 2003). However, in general, halogens will strongly partition into a fluid phase compared to a melt (Bureau et al. 2000). Therefore, in this review, the focus is on halogen transport via fluids from the dehydrating slab. In addition, the use of halogen ratios and halogen isotopes to trace slab-derived fluid sources has traditionally assumed transport through the mantle wedge in a near vertical manner and therefore outputs across the arc represent depth to the subducting slab. This assumption ignores potential complications due to non-vertical transport along the slab-mantle interface and within the mantle wedge (Hoernle et al. 2008; Marschall and Schumacher 2012).

**Fig. 8.1** **a** F/Cl versus I/Cl and **b** Br/Cl versus I/Cl of various subduction-zone reservoirs (modified from John et al. 2011; Kendrick et al. 2014a). Arc lava and subducting sediment data from John et al. (2011). F/Cl back arc basalt (BABB) glass data from Bézou et al. (2009); Br/Cl and I/Cl BABB data from Kendrick et al. (2014a). Serpentinite data in **a** from John et al. (2011) and in **b** from Kendrick et al. (2013). The I concentration in altered oceanic crust (AOC) is unknown. Here we assume it to be lower than that of MORB (Kendrick et al. 2014a). Halogen ratios of sedimentary pore fluids from Fehn et al. (2006, 2007), Muramatsu et al. (2001) and references therein



volcanoes have Cl concentrations up to  $\sim 5800 \mu\text{g/g}$  (St. Augustine, Aleutians; Zimmer et al. 2010) and F concentrations up to  $\sim 2500 \mu\text{g/g}$  (Irazú, Central America; Benjamin et al. 2007). Although halogens are extremely hydrophilic, there is increasing evidence that they may survive within the slab past the arc volcanic front despite extensive slab dehydration ( $\sim 65\%$  global average of water loss by subarc depths; Hacker 2008). Recent work has also shown halogen enrichment in back-arc basalts and ocean-island basalts compared to MORB (e.g., Kendrick et al. 2012b, 2014a, b; Kent et al. 2002; Sun et al. 2007).

Here we review halogen reservoirs, movement, and geochemistry in subduction systems. We begin by providing an overview of the concentrations of halogens in inputs (pore fluids, sediments, altered oceanic crust, and serpentinites) into the subduction system and how these halogens are lost during subduction zone metamorphism. Halogen concentrations in outputs (volcanic gas and melt inclusions) are summarized, allowing for calculations to be made of halogen flux through the volcanic front and evidence of halogen transport into the upper mantle. We also discuss the role halogens have on subduction-zone fluid chemistry and the transport of metals and trace elements. Finally, we discuss the use of halogen isotopes as tracers of volatile sources in subduction zones.

## 8.2 Halogen Sources into the Subduction Zone

### 8.2.1 Pore Fluids

It is estimated that pore fluid in subducted sediments and altered oceanic crust (AOC) accounts for  $\sim 60\%$  of the total water entering subduction zones (Jarrard 2003). Pore fluids are enriched in halogens, especially I (Kastner et al. 1991; Martin et al. 1993; Muramatsu et al. 2007). This I enrichment is due to the breakdown of organic sediments during diagenesis with some samples having I concentrations  $>100 \mu\text{g/g}$  (Fehn et al. 2007; Martin et al. 1993; Muramatsu et al. 2001; Snyder et al. 2005; Tomaru et al. 2007). These high concentrations are well above the seawater concentration of  $55 \text{ ng/g}$  (Geochemical Reference Model, [earthref.org/GERM](http://earthref.org/GERM)). In general, the Br concentration in pore fluids ranges from near that of seawater to twice the concentration of seawater (Fehn et al. 2007; Martin et al. 1993; Muramatsu et al. 2007). Chlorine concentrations are also high, ranging from near seawater concentration ( $\approx 19,500 \mu\text{g/g}$ ) to about 50% of seawater concentration (Kastner et al. 1991; Mottl et al. 2004). Sedimentary pore fluids have Br/Cl ratios of 0.0035–0.009 and I/Cl ratios of 0.000003–0.01 (both ratios are characteristically higher than that of seawater) (Kendrick et al. 2014b) (Fig. 8.1). To our knowledge, little work has been done to determine F concentrations in pore fluids.

It is commonly assumed that pore fluids are expelled at shallow levels in subduction zones (by  $\sim 5 \text{ km}$  depth) due to porosity collapse and compaction (e.g., Jarrard 2003; Kastner et al. 1991; van Keken et al. 2011). Pore fluids are thus typically ignored in elemental budgets of subduction zone cycling. Some work suggests that pore fluids may survive to  $\sim 100 \text{ km}$  depth in subduction zones, based on noble gas and high I/Cl and Br/Cl ratios in fluid inclusions in a mantle wedge peridotite (Sumino et al. 2010). However, recent studies have shown that serpentinites are a large, hitherto unknown sink of I and that high I/Cl and Br/Cl ratios in fore-arc serpentinites can explain these halogen trends in fluid inclusions (Kendrick et al. 2011, 2013). There are two different interpretations regarding pore fluid interaction with serpentinites: (1) pore fluids serpentinize peridotite under low-T as a result of fluid infiltration in a bending fault in outer rise settings (John et al. 2011; Kendrick et al. 2011), or (2) pore fluids are squeezed from the compacting sediment and infiltrate the peridotite above the subduction channel, driving low-T serpentinization (Kendrick et al. 2011; Scambelluri and Tonarini 2012). These elements are then recycled in high-pressure fluids without the need to subduct pore fluids to  $100 \text{ km}$  (Kendrick et al. 2011, 2013).

### 8.2.2 Sediments

Estimates of Cl and F concentration in marine sediments vary widely. Measured Cl concentrations in marine sediments (e.g., hemipelagic mud, marls, pelagic clay)

from various DSDP/ODP/IODP drill sites range from  $\sim 40$  to  $\sim 2000$   $\mu\text{g/g}$  (Barnes et al. 2008, 2009b; John et al. 2011) and F concentrations range from  $\sim 400$  to  $\sim 1250$   $\mu\text{g/g}$  (John et al. 2011). Ito et al. (1983) used a Cl concentration of 1200  $\mu\text{g/g}$  in clays and carbonates to calculate that  $3.2 \times 10^{12}$  g of Cl are subducted globally each year in marine sediments. Subsequent flux estimates of Cl and F derived from subducting sediments, are based on their average concentration in the upper continental crust (Cl = 640  $\mu\text{g/g}$  and F = 611  $\mu\text{g/g}$ ; Gao et al. 1998; Wedepohl 1995), resulting in the estimate that  $1.6 \times 10^{12}$  g of Cl and  $1.5 \times 10^{12}$  g of F are globally subducted in sediments each year (John et al. 2011; Straub and Layne 2003).

70% of the Earth's I is hosted in marine sediments due to the accumulation of I in organic material (Muramatsu and Wedepohl 1998). Estimated and measured I concentrations in marine sediments range from  $<1$  to 28  $\mu\text{g/g}$  (John et al. 2010; Li and Schoemaker 2003; Muramatsu et al. 2007; Muramatsu and Wedepohl 1998). Muramatsu and Wedepohl (1998) estimate 30 ppm I in marine carbonates. Because I concentrations in marine sediments are directly linked to the presence of organic material and because most subducting sediments were deposited under deep sea conditions, sediments entering the subduction system are likely to have I concentrations near the lower end of this range (Fehn 2012). If one uses 5  $\mu\text{g/g}$  I in subducting marine sediments, then an estimated  $1.2 \times 10^{10}$  g of I in marine sediments is subducted annually.<sup>2</sup>

Bromine concentrations in marine sediments are poorly known. Li (1982) estimates concentrations of 70  $\mu\text{g/g}$  in marine pelagic clays. Analyses of marine sediments indicate that values range from 0.3 to 70  $\mu\text{g/g}$  Br (John et al. 2011; Muramatsu et al. 2007). Using 20  $\mu\text{g/g}$  Br (average of values reported in John et al. (2011) and Muramatsu et al. (2007)), an estimated  $4.9 \times 10^{10}$  g of Br is subducted annually in marine sediments.

With the exception of I, little work has been done on halogen loss from sediments during subduction. Data from metasedimentary gneisses, mica schists, and granulites show that sediments likely lose 75 to 95% of their I by about 400 °C (Muramatsu and Wedepohl 1998). Iodine enrichment in fore-arc waters and gases is largely due to the loss of I from marine sediments during the early stages of subduction (e.g., Muramatsu et al. 2001; Tomaru et al. 2007). Despite the ability of sediments to host large amounts of halogens, sediments constitute a relatively small percentage of the subducted material and, in the case of I, halogens may be lost from sediments early in the subduction process.

---

<sup>2</sup>For consistency and ease of comparing input fluxes, all calculated fluxes in this contribution use the parameters outlined in Straub and Layne (2003) and John et al. (2011): convergence rate of 5 cm/yr, bulk crust density of 2.8 g/cm<sup>3</sup>, 44,000 km of trench length, 400 m thickness of sediment, 6 km thickness of AOC, and 5% serpentinization of the upper 6 km of lithospheric mantle (or 100% serpentinization of 300 m) to 15% serpentinization of the upper 3 km of lithospheric mantle (or 100% serpentinization of 450 m).

### 8.2.3 Altered Oceanic Crust (AOC)

Most work on halogen concentrations in AOC has focused on Cl and to a lesser extent F. However, Cl and F concentrations in AOC remain poorly constrained due to limited accessibility of the deeper crust; scarcity of Cl and F abundance data of bulk rock and secondary minerals in the literature; and the chemical heterogeneity of the crust (Straub and Layne 2003). Metasomatism of oceanic crust results in the formation of secondary hydrous minerals (e.g., clays, chlorite, amphiboles, talc, epidote), which can incorporate Cl and F into their mineral structure (e.g., Ito et al. 1983; Philippot et al. 1998; Vanko 1986). Amphibole is commonly assumed to be the major sink for Cl and F in AOC. Chlorine concentrations of amphibole range from below electron microprobe detection limits (typically  $\sim 0.01$  wt%) to as high as 4 wt% (Gillis 1996; Gillis and Meyer 2001; Ishizuka 1989; Laverne et al. 1995; Pertsev et al. 2015; Vanko 1986; Vanko and Stakes 1991); whereas F concentrations range from below electron microprobe detection limits (typically  $\sim 0.2$  wt%) to as high as 0.54 wt% (Gillis 1996; Gillis and Meyer 2001; Vanko 1986). Estimates of the Cl concentration in AOC, based on assumed Cl concentrations and modal abundances of secondary minerals, range from 50 to 78  $\mu\text{g/g}$  Cl (Ito et al. 1983; Straub and Layne 2003). These values yield an estimated  $2.5$  to  $2.9 \times 10^{12}$  g of Cl in AOC subducted globally each year (Ito et al. 1983; Jarrard 2003). Analyses of bulk Cl concentrations in AOC are limited to three studies (Barnes and Cisneros 2012; Bonifacie et al. 2007a; Sano et al. 2008). Barnes and Cisneros (2012) propose 207  $\mu\text{g/g}$  Cl in AOC based on a weighted average of bulk Cl concentrations in extrusive lavas, sheeted dikes, and gabbros from seven DSDP/ODP/IODP drill sites for a subducted Cl budget of  $8.1 \times 10^{12}$  g/yr from AOC. Bulk-rock Cl contents in eclogite-facies AOC rocks range from 10 to 95  $\mu\text{g/g}$  (Marschall et al. 2009; Selverstone and Sharp 2013); bulk Cl concentrations determined from Cl concentrations in eclogite-facies minerals yield similar estimates (71–79  $\mu\text{g/g}$ ; Debret et al. 2016). Most of the Cl is hosted in amphiboles, with smaller amounts contained in chlorite, talc, chloritoid, garnet, and omphacite (Debret et al. 2016; Selverstone and Sharp 2013). Calculated F concentration for AOC, based on F concentrations in minerals, is 216  $\mu\text{g/g}$  with an estimated  $8.0 \times 10^{12}$  g of F in AOC globally subducted each year (John et al. 2011; Straub and Layne 2003). Bulk F concentrations in eclogite-facies AOC, also based on F concentrations in minerals, ranges from 10 to 16  $\mu\text{g/g}$ , suggesting loss of F to the fore-arc from amphibole breakdown (Debret et al. 2016).

The Br and I content of AOC is virtually unknown. Muramatsu and Wedepohl (1998) estimate that AOC hosts about 9 ng/g I (nearly identical to the I concentration in MORB, see Sect. 8.5.1) based on analyses of bulk mafic rock. This suggests that a calculated  $3.3 \times 10^8$  g of I in AOC are globally subducted each year. Kendrick et al. (2014a) hypothesized that AOC has lower Br/Cl and I/Cl ratios than MORB due to hydrothermal alteration, which increases the Cl concentration in AOC. They suggest a Br/Cl of  $<0.0025$ , but do not speculate on the I/Cl ratio

(Kendrick et al. 2014a) (Fig. 8.1). For our flux calculations (Table 8.1), we use a Br concentration of 150 ng/g. This value is based on Br concentrations in MORB (see Sect. 8.5.1) and is consistent with the Br/Cl ratio used by Kendrick et al. (2014a).

Fluids released by amphibole breakdown were long thought to be the primary fluid source for arc magmatism and the control on the location of the volcanic front (Davies and Stevenson 1992; Tatsumi 1986; Tatsumi and Eggins 1995). Additionally, amphibole breakdown may produce the Cl-rich fluids found in eclogites (Philippot and Selverstone 1991). However, experimental constraints indicate that equilibrium amphibole breakdown occurs at shallower depths than most arc volcano fronts, so amphibole-derived, Cl-rich fluids likely primarily affect the forearc mantle (Schmidt and Poli 1998). Therefore, a slab-derived saline fluid source which is stable to greater depths in a subduction zone is needed to account for the transport of Cl to sub-arc depths (e.g., Scambelluri and Philippot 2001).

### 8.2.4 *Serpentinites*

In the last 20 years, it has become clear that serpentinites play a key role in the transport of water, carbon, fluid-mobile elements (FME; e.g., B, As, Sb, Li, Pb), and halogens into subduction zones. Serpentinites form via the hydration of mantle rocks in different geodynamic environments (Fig. 8.2a) and host up to 13 wt% water. Historically, serpentinite formation was attributed to seawater-driven alteration of mid-ocean ridge mantle. Such abyssal serpentinites are more widespread in modern slow- and ultraslow-spreading oceans, where they can cover 25% of the seafloor (Cannat et al. 1995). Past Alpine subduction largely involved this type of oceanic lithosphere (Lagabrielle and Cannat 1990). In fast spreading oceans, like the present-day Pacific, a thick crustal layer prevents seawater interaction with deep-seated mantle peridotite, unless transform faults and bend faults at outer rises (Fig. 8.2a) enable deep seawater infiltration and mantle serpentinization (Kerrick 2002; Ranero et al. 2003). The extent of mantle serpentinization within bend faults has yet to be properly quantified. At convergent plate margins, rising slab fluids form kilometer-thick serpentinite layers in the supra-subduction forearc mantle (Bostock et al. 2002; Hyndman and Peacock 2003; Rüpke et al. 2004; Savov et al. 2005; Tatsumi 1989).

Serpentine (antigorite) stability over a large pressure range provides a means to transport water and FME to depths of 150–200 km (Fig. 8.2b) (Ulmer and Trommsdorff 1995; Wunder and Schreyer 1997), thus affecting global geochemical cycles (e.g., Barnes and Straub 2010; Cannao et al. 2015; Deschamps et al. 2013; Luth 2014; Ryan and Chauvel 2014; Scambelluri et al. 1997, 2004; Scambelluri and Tonarini 2012; Schmidt and Poli 1998; Straub and Layne 2003). In addition, the trace element and rare earth element (REE) compositions of serpentinites can be used to fingerprint the tectonic setting of formation and the fluid-rock interactions occurring during subduction (Fig. 8.2a) (Deschamps et al. 2013; Kodolányi et al. 2012). Compared to abyssal serpentinites from mid-ocean ridges, the geochemistry

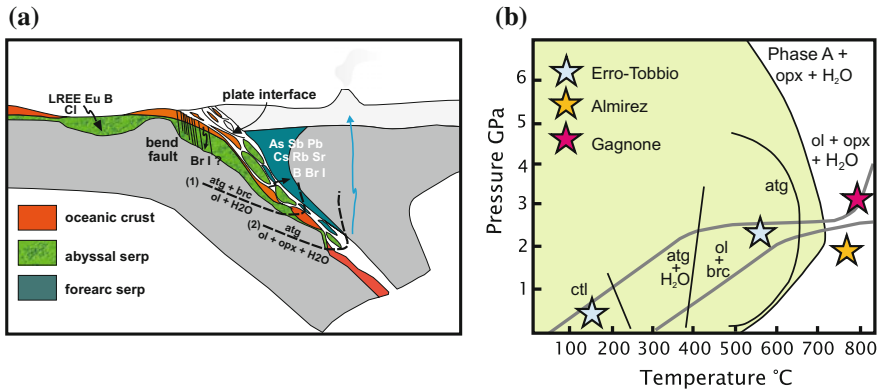


**Fig. 8.2** **a** Schematic sketch (not to scale) showing serpentinite from various environments: (1) abyssal serpentinite, (2) bend-fault serpentinite, and (3) forearc mantle serpentinite. Also shown are subducting serpentinites and the plate interface subduction channel and the possible fluxes of elements in abyssal and forearc serpentinites (after Deschamps et al. 2013). Still unknown is the effective elemental influx related to bend faults. The hypothesized flux shown here in bend faults is after John et al. (2011) and Kendrick et al. (2011). Serpentinite in the subduction plate interface becomes enriched in a comparable set of elements as the forearc serpentinite (Cannaò et al. 2015; Deschamps et al. 2013; Scambelluri et al. 2014). **b** P-T diagram showing the stability field of chrysotile, antigorite + brucite, antigorite, and olivine + orthopyroxene assemblages. The stability of antigorite is influenced by the Al content that shifts antigorite stability to higher T (Ulmer and Trommsdorff 1995). Model subduction-zone gradients at the top of the slab from Syracuse et al. (2010) are represented by the *dark grey curves*. The subduction zone gradients reported here correspond to the ones shown in Fig. 8.10. The *stars* indicate the P-T crystallization conditions of Erro-Tobbio (shallow serpentinitization overprinted by high-pressure recrystallization) (Scambelluri et al. 2004), Almiraz (Trommsdorff et al. 1998) and Gagnone (Scambelluri et al. 2014). Abbreviations: *atg* antigorite, *brc* brucite, *ol* olivine, *opx* orthopyroxene

of serpentinites from convergent margins suggests significant involvement of sedimentary material, either present on top of the bending faults or in the subduction channel, located at the interface between the subducting and the overriding plates (Fig. 8.2a) (Deschamps et al. 2013; John et al. 2011; Kendrick et al. 2011; Lafay et al. 2013; Scambelluri et al. 2014).

The uptake of water, C, FME, and halogens into serpentinites and the cycling of these elements during subduction can be determined using coupled field and geochemical studies of serpentinites recording P-T conditions from shallow to deep levels within subduction zones. Low-P and low-T ( $T < 300$  °C; Fig. 8.2b) serpentinitization generally produces lizardite and/or chrysotile pseudomorphs (with variable amounts of chlorite, magnetite + talc, actinolite) after the primary mantle minerals (Fig. 8.3a). During subduction, fluids and elements are lost from serpentinite during the chrysotile-antigorite transition (Kodolányi and Pettke 2011) and via the following prograde dehydration reactions:

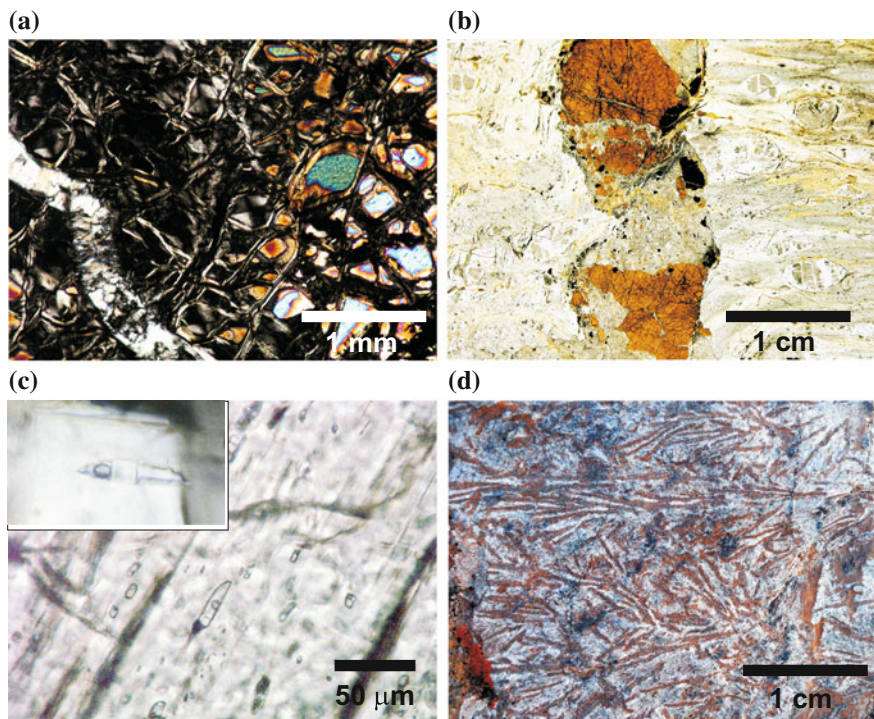
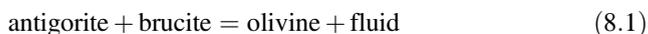


**Fig. 8.3** **a** Shallow Erro-Tobbio serpentinite showing serpentine after mantle olivine (present as relict grains in a mesh serpentine texture). Chrysotile is cut by an antigorite vein (left corner of the picture). Crossed nicols. **b** Ti-clinohumite (red), olivine (white), minor diopside, and magnetite vein in a foliated Erro-Tobbio antigorite serpentinite with clasts of relict mantle clinopyroxene. The vein is a dehydration fluid conduit. **c** Fluid inclusions in diopside from an Erro-Tobbio vein. The inclusions contain H<sub>2</sub>O liquid, a vapour bubble and salt (NaCl and MgCl) daughter crystals (visible in the inset). **d** Olivine (brown elongate crystals) and orthopyroxene + chlorite (grey areas in between olivine) from an Almiraz spinifex chlorite harzburgite, which derived from antigorite breakdown. The recrystallization conditions of the rocks reported here are shown by the yellow and red stars in Fig. 8.2b (i.e., the peak P-T conditions of Gagnone and Almiraz chlorite harzburgites)



and



Reaction (8.1) involves dehydration of antigorite and brucite and leads to consumption of the less abundant reactant (brucite) to produce metamorphic olivine and fluid (Fig. 8.2b). It is recorded by most eclogite-facies Alpine serpentinites (e.g., Erro-Tobbio and Lanzo peridotite, Western Alps), showing rock- and vein-forming antigorite + olivine-bearing parageneses overgrowing early generations of low-T

chrysotile serpentine (Fig. 8.3b) (Debret et al. 2013; Scambelluri et al. 1995, 1997). Pressure-temperature estimates of the Alpine eclogites coexisting with olivine-bearing high-pressure serpentinite yield estimates in the range of 2–2.5 GPa, indicating that reaction (8.1) occurs at approximately 80 km depths (Angiboust et al. 2009, 2012; Bucher et al. 2005; Hermann et al. 2000; Li et al. 2004; Pelletier and Müntener 2006; Rebay et al. 2012). The fluid produced at this stage is preserved as salty aqueous inclusions in veins (Fig. 8.3c) (Scambelluri et al. 1997). Although the high salinity of this fluid may be caused by fluid/rock interaction before and/or during inclusion entrapment, this evidence demonstrates recycling of Cl and associated halogens in subduction fluids (Scambelluri et al. 2004). A larger amount of fluid is released by reaction (8.2), experimentally reproduced at pressure-temperature conditions which may range, depending on subduction gradients, from subarc (110 km) to 200 km depths (Ulmer and Trommsdorff 1995; Wunder and Schreyer 1997). Reaction (8.2) is recorded in two localities: Cerro del Almirez (SE Spain) and Cima di Gagnone (Swiss Central Alps) (Evans and Trommsdorff 1978; Scambelluri et al. 2014; Trommsdorff et al. 1998). These rocks display olivine, orthopyroxene and chlorite in spinifex-like or in a granular equilibrium texture (Fig. 8.3d) (Padrón-Navarta et al. 2010; Scambelluri et al. 2014). These dehydrated serpentinites also preserve relics of the fluid phase released during antigorite breakdown in the form of solid polyphase inclusions hosting an aqueous liquid phase (Scambelluri et al. 2001).

Serpentinites are major hosts of Cl and I (Fig. 8.2a) (Barnes and Sharp 2006; Debret et al. 2014; John et al. 2011; Kendrick et al. 2011, 2013; Scambelluri et al. 1997, 2004; Sharp and Barnes 2004). Abyssal serpentinites have average Cl concentrations of  $\sim 2000$   $\mu\text{g/g}$  structurally bound in serpentine (Anselmi et al. 2000; Barnes and Sharp 2006; Kendrick et al. 2013; Kodolányi and Pettke 2011; Sharp and Barnes 2004). Fluorine concentrations in serpentinites are rarely reported, but average around 204  $\mu\text{g/g}$  (Mével 2003; Stueber et al. 1968). Only recently have Br and I concentrations been measured in serpentinites (Kendrick et al. 2011, 2013), with Br and I concentrations in seafloor and forearc serpentinites of 1.3–24  $\mu\text{g/g}$  (average = 6.4  $\mu\text{g/g}$ ) and 0.02–45  $\mu\text{g/g}$  (average = 7.6  $\mu\text{g/g}$ ), respectively. Figure 8.4a shows the Br/Cl versus I/Cl ratios of serpentinites from modern mid-ocean ridges, passive and convergent plate margins, along with ophiolitic peridotites serpentinitized in shallow settings (Internal and External Liguride Ophiolites, Apennine, and part of Erro-Tobbio, Alps; data after Kendrick et al. 2013; John et al. 2011). I/Cl and Br/Cl ratios in serpentinites are similar to ratios of sedimentary marine pore fluids (Figs. 8.1b and 8.4a), implying a contribution of pore fluids to the serpentinitizing fluid. The Br and I contents of these rocks increase relative to Cl from abyssal to forearc serpentinites. This is likely a result of the involvement of a (meta)sedimentary component in the serpentinitization fluids due to the loss of fluids from sediments at shallow depths within the subduction zone hydrating the forearc mantle wedge. Interestingly, the Northern Apennine ophiolitic serpentinites that escaped subduction show significantly higher Br and I than modern abyssal serpentinites. High Br and I concentrations are also recorded in early chrysotile relics preserved in the subducted Erro-Tobbio unit.

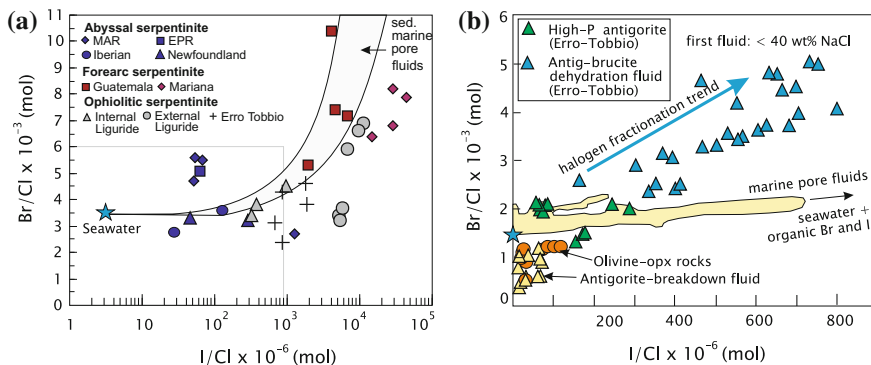


**Fig. 8.4** **a** Br/Cl versus I/Cl element plots showing chrysotile–lizardite serpentinites from abyssal (Mid Atlantic Ridge, MAR; East Pacific Rise, EPR; Iberian and Newfoundland), forearc (Guatemala and Mariana), and ophiolitic settings (Internal and External Liguride, Northern Apennine; Erro-Tobbio, Alps). Reference fields include the compositional range of sedimentary marine pore fluids and of seawater (modified from Kendrick et al. 2013; data from Kendrick et al. 2013; John et al. 2011). **b** inset of Fig. 8.4a (light grey line) showing the compositions of high-pressure antigorite and saline fluid inclusions from Erro-Tobbio (released from reaction 8.1 in Fig. 8.2b; see for instance Fig. 8.3d) together with the compositions of the Almiraz harzburgites and associated fluid inclusions (released from reaction 8.2 in Fig. 8.2b). The field of sedimentary pore fluids is also reported (after Kendrick et al. 2011)

This geochemical feature indicates the involvement of sedimentary marine pore fluids during shallow serpentinization of these mantle rocks (Kendrick et al. 2013). These data lead to the conclusion that shallow serpentinization took place in outer rises, accretionary complexes, or in the mantle wedge (i.e., settings quite distant from mid ocean ridges) (Kendrick et al. 2011, 2013; John et al. 2011; Scambelluri and Tonarini 2012). A contribution of pore fluids to the serpentinizing fluid is also supported by noble gas data (Kendrick et al. 2011) and Cl isotope data (Barnes et al. 2006; Barnes and Sharp 2006).

Halogens can be lost (up to 90% of Cl) during the chrysotile-to-antigorite transition during the early stages of subduction (<30 km) (Kodolányi and Pettke 2011). However, work on exhumed high-pressure serpentinites shows that despite progressive dehydration and halogen loss during the early stages of subduction, high-pressure serpentinites retain significant concentrations of halogens (Bonifacie et al. 2008a; John et al. 2011; Scambelluri et al. 2004; Selverstone and Sharp 2013). The extent of Cl recycling during serpentinite subduction is illustrated in Fig. 8.5, which shows the concentrations measured in minerals crystallized at increasing pressure-temperature conditions. Here the Erro-Tobbio and Almiraz subducted units record dehydration reactions (8.1) and (8.2), respectively (see Fig. 8.2b for P-T equilibration conditions; Scambelluri et al. 2004). Subduction results in a decrease in Cl and B concentrations in minerals due to the progressive release of such elements into the fluids. The estimated bulk-rock Cl budgets are shown in Fig. 8.5b. Overall, Fig. 8.5 shows that, despite Cl and B loss to subduction fluids,

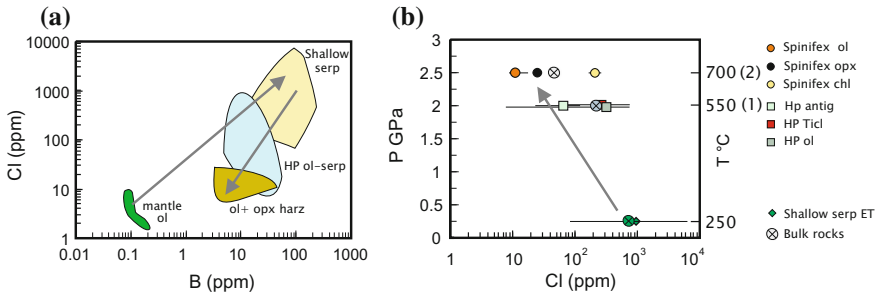


**Fig. 8.5** **a** Boron versus Cl composition of mantle olivine, early shallow chrysotile, and high-pressure minerals in olivine-serpentinite formed after reaction (8.1), and in deserpentinized olivine + orthopyroxene + chlorite harzburgite formed after reaction (8.2). Data are from the Erro-Tobbio high-pressure serpentinite and in the Almirez chlorite harzburgite (Scambelluri et al. 2004). **b** Mineral and bulk-rock Cl variability in the above samples as a function of the estimated metamorphic pressures and temperatures and the reference reactions (8.1) and (8.2)

the most dehydrated rocks still retain appreciable amounts of such elements. Detailed variations in the halogen compositions from subduction-zone serpentinite and fluids from Erro-Tobbio and Almirez are shown in Fig. 8.4b. In general, the residual high-pressure serpentinites show decreasing concentrations of Cl, Br, and I with increasing dehydration (John et al. 2011; Kendrick et al. 2011). In samples from Almirez, the above scenario is complicated by the recently documented exchange of radiogenic Sr and  $^{11}\text{B}$  between ultramafic rocks and the surrounding metasediments during subduction (Harvey et al. 2014). This suggests caution when reconstructing element loss from these rocks compared with other units evolved at different pressure-temperature conditions. However, the constant halogen loss between Erro-Tobbio and Almirez (Fig. 8.5) and the halogen variations shown in Fig. 8.4b encourage the use of these rocks to assess halogen behavior during serpentinite subduction.

Halogen loss from subducting serpentinite is counterbalanced by increased halogen concentrations in veins and in fluid inclusions, suggesting that halogens are preferentially released to the fluid during dehydration. The variation between rock residues and fluids is shown by the halogen fractionation trend in Fig. 8.4b (John et al. 2011; Kendrick et al. 2011), with Br and I progressively depleted relative to Cl (Kendrick et al. 2011). Interestingly, the halogen signature of the Erro-Tobbio high-pressure antigorite serpentinite, formed after shallow-level chrysotile serpentinite (see Fig. 8.4a), can be tracked back to the original marine pore fluid signature (Fig. 8.4b). With increasing grade, F/Cl ratios increase in the residual rock (John et al. 2011). This increase in F may be due to the formation of Ti-clinohumite (John et al. 2011), which is able to host large concentrations of F with increasing metamorphic grade (Evans and Trommsdorff 1983; Lopez Sánchez-Vizcaíno et al. 2005), as evidenced by correlations between F and Ti concentrations.

Overall, Fig. 8.5 shows that, despite Cl and B loss to subduction fluids, the most dehydrated rocks still retain appreciable amounts of such elements.

The rock forming olivine, orthopyroxene and chlorite from the Almirez chlorite harzburgite contain 10  $\mu\text{g/g}$  Cl on average, which corresponds to an average bulk estimate of 40  $\mu\text{g/g}$  Cl (Fig. 8.5b; Scambelluri et al. 2004). Bulk analyses of such rocks show that they can contain up to  $\sim 250$   $\mu\text{g/g}$  Cl,  $\sim 40\text{--}50$   $\mu\text{g/g}$  F, 0.2  $\mu\text{g/g}$  Br, and  $\sim 700$  ng/g I (John et al. 2011; Kendrick et al. 2011), thus introducing detectable halogen anomalies into the upper mantle.

### 8.3 Halogen Outputs from the Subduction Zone

Halogens are recycled to the Earth's surface through the forearc, volcanic front, and the backarc. Fluxes through the fore-arc are very poorly constrained, in part due to limited accessibility of venting fore-arc gases and fluids, and therefore are ignored in all published volatile cycling budgets (e.g., Ito et al. 1983; Jarrard 2003; John et al. 2011; Straub and Layne 2003; Wallace 2005). In this section, we focus on the better constrained halogen fluxes through the volcanic arc from measurable halogen concentrations in volcanic gases and melt inclusions.

#### 8.3.1 Volcanic Gas Data

Halogen concentrations in gas plumes are determined using halogen to  $\text{SO}_2$  ratios and  $\text{SO}_2$  flux measurements.  $\text{SO}_2$  is the most commonly measured gas because of its high abundances in volcanic plumes, low atmospheric background and strong absorption in UV (e.g., Fischer 2008; Wallace 2005). Improvements in  $\text{SO}_2$  flux measurements will therefore result in better quantification of other gas fluxes.  $\text{SO}_2$  flux measurements have traditionally been made using the ground-based UV correlation spectrometer (COSPEC). More recently, rapid advances have been made in  $\text{SO}_2$  flux measurements using UV spectrometry by application of differential optical absorption spectrometry (Shinohara 2008) and satellite remote sensing techniques (Pieri 2015).

Halogens are commonly degassed as hydrogen halides (HCl, HF, HBr, HI) (Aiuppa et al. 2005; Symonds et al. 1988), although other trace halogen compounds are possible (e.g., BrO, ClO) (Bobrowski et al. 2003; Platt and Bobrowski 2015). Measurements of Cl and F concentrations in volcanic gases are not common and those of Br and I are rare (Aiuppa et al. 2005, 2009; Fischer 2008; Snyder and Fehn 2002). Despite the limited concentration data in the literature, several studies have attempted to estimate the halogen flux from arc volcanoes based on volcanic gas data (Table 8.1). Errors associated with these estimates reflect possible modification of halogen concentrations during transport from the magma to the surface, limited data from some arcs, and how to “scale up” to an estimation of total arc volcanic output starting with variable halogen concentrations among fumaroles at an individual volcano (Fischer 2008; Pyle and Mather 2009). In addition, with the

**Table 8.1** Calculated input and output budgets for various reservoirs

<i>Calculations from this contribution<sup>a</sup></i>										
	Thickness (m)	Cl (ppm)	F (ppm)	I (ppb)	Br (ppm)	Subduction influx (g Cl/yr)	Subduction influx (g F/yr)	Subduction influx (g I/yr)	Subduction influx (g Br/yr)	
Sediments	400	640	611	5000	20	$1.6 \times 10^{12}$	$1.5 \times 10^{12}$	$1.2 \times 10^{10}$	$4.9 \times 10^{10}$	
Altered oceanic crust	6000	207	216	9	0.15	$7.7 \times 10^{12}$	$8.0 \times 10^{12}$	$3.3 \times 10^8$	$5.5 \times 10^9$	
Serpentinites	300–450	2000	204	7600	6.4	$3.7\text{--}5.5 \times 10^{12}$	$3.8\text{--}5.7 \times 10^{11}$	$1.4\text{--}2.1 \times 10^{10}$	$1.2\text{--}1.8 \times 10^{10}$	
<b>Total</b>						<b><math>13\text{--}15 \times 10^{12}</math></b>	<b><math>9.9\text{--}10 \times 10^{12}</math></b>	<b><math>2.6\text{--}3.3 \times 10^{10}</math></b>	<b><math>6.7\text{--}7.3 \times 10^{10}</math></b>	
<i>Prior work<sup>b</sup></i>										
Straub and Layne (2003)						Subduction influx (g Cl/yr)	Subduction influx (g F/yr)	Subduction influx (g I/yr)	Subduction influx (g Br/yr)	
Ito et al. (1983)						$3.7 \times 10^{12}$	$7.9 \times 10^{12}$			
Jarrard (2003)						$3.6\text{--}8.6 \times 10^{12}$				
Snyder and Fehn (2002)						$4.5 \times 10^{12}$		$2.0 \times 10^{10}$		
Jarrard (2003)						Arc outflux (g Cl/yr)	Arc outflux (g F/yr)	Arc outflux (g I/yr)	Arc outflux (g Br/yr)	
Straub and Layne (2003)						$7\text{--}22 \times 10^{12}$				
Ito et al. (1983)						$2.9\text{--}3.8 \times 10^{12}$	$0.3\text{--}0.4 \times 10^{12}$			
Wallace (2005)						$4.3\text{--}9.5 \times 10^{12}$				
Ruscitto et al. (2012)						$4\text{--}7 \times 10^{12}$				
						$5.6 \times 10^{12}$				

(continued)

**Table 8.1** (continued)

<i>Calculations from this contribution<sup>a</sup></i>									
	Thickness (m)	Cl (ppm)	F (ppm)	I (ppb)	Br (ppm)	Subduction influx (g Cl/yr)	Subduction influx (g F/yr)	Subduction influx (g I/yr)	Subduction influx (g Br/yr)
Pyle and Mather (2009)						$4.2 \times 10^{12}$	$0.5 \times 10^{12}$	$0.5-2 \times 10^9$	$4.9-14.8 \times 10^9$
Fischer (2008)						$5.5 \times 10^{12}$	$0.2 \times 10^{12}$		
Shinohara (2013)						$1.1 \times 10^{13}$			

<sup>a</sup>Details for calculations and references for values used are summarized in the text in Sect. 8.2

<sup>b</sup>None of the prior influx calculations for any halogen includes contributions from serpentinites or pore fluids. Arc outflux estimates are based on gas data with the exception of Straub and Layne (2003) and Ruscitto et al. (2012), which are based on volatile contents in magma (melt inclusion data) and magma production rates. Shinohara (2013) is the only estimate to include volatile data from thermal spring discharge

exception of Shinohara (2013), none of these estimates include halogen fluxes through thermal springs, which may be significant (e.g., Taran 2009). Instead, they focus solely on high temperature fumarole fluxes (Fischer 2008; Pyle and Mather 2009). Despite these possible errors, the estimated outputs are remarkably consistent, especially given that some of the estimates are based on volcanic gas data (e.g., Fischer 2008; Pyle and Mather 2009) and others on melt inclusion data (Ruscitto et al. 2012; Straub and Layne 2003).

### 8.3.2 Melt Inclusions

The last ~15 years have seen a rapidly growing database of halogen contents in melt inclusions<sup>3</sup> (e.g., Wallace 2005), including those from arc volcanoes (e.g., Cervantes and Wallace 2003; Esposito et al. 2014; Johnson et al. 2009; Portnyagin et al. 2007; Ruscitto et al. 2010; Sadofsky et al. 2008; Shaw et al. 2008). Halogen contents are enriched in arc lavas compared to MORB (Fig. 8.6) and this enrichment is commonly cited as strong evidence for the contribution of slab-derived fluids to arc volcanism (e.g., Wallace 2005). The highest Cl concentrations reported in olivine-hosted melt inclusions from arc basalts are ~5800 µg/g from Augustine in the Aleutian arc (Fig. 8.6a) (Zimmer et al. 2010). Published F data are sparse, but include concentrations up to ~2500 µg/g from Irazú (Fig. 8.6b) (Benjamin et al. 2007). Due to the high solubility of Cl and F in mafic (basaltic) melts (e.g., Webster et al. 1999) and no diffusive re-equilibration of Cl and F through host olivine (Bucholz et al. 2013), these values are believed to reflect initial melt compositions (e.g., Benjamin et al. 2007; Wade et al. 2006). Reported Br concentrations in melt inclusions is limited to Central America with concentrations up to 13 µg/g (Kutterolf et al. 2013). To our knowledge, there are no published data on I concentrations in melt inclusions.

Chlorine contents in many arc basalts have been explained by mixing between a mantle source and slab-derived fluid with a Cl/H<sub>2</sub>O ratio similar to that of seawater (Johnson et al. 2009; Ruscitto et al. 2010; Wallace 2005). Many melt inclusions from arc samples have Cl/H<sub>2</sub>O ratios consistent with the salinity of a fluid derived from serpentinites (4–8 wt% NaCl) (Scambelluri et al. 2004) or altered oceanic crust (~4 wt% NaCl for the upper crust and ~35 wt% for the lower crust) (Nehlig 1993; Philippot et al. 1998) (cf., Johnson et al. 2009). Volcanic magmas with

---

<sup>3</sup>For purposes of comparison, only olivine melt inclusion data from arc basalts are presented and discussed; however, melt inclusions from other mineral phases (e.g., plagioclase) and volcanic glass shards also provide viable and valuable data. For example, Balcone-Boissard et al. (2010) show that Cl/Br/I ratios are constant in pumice from felsic explosive eruptions, suggesting that these halogens are not fractionated from each other during rapid magma decompression and can be used to trace mantle source compositions.

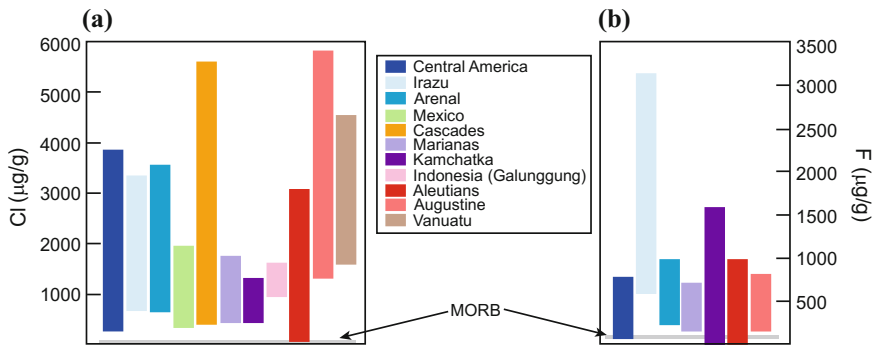


**Fig. 8.6** **a** Cl and **b** F concentrations in olivine-hosted melt inclusions from arc basalts. Fields enclose data from Central America (Benjamin et al. 2007; Kutterolf et al. 2013; Roggensack et al. 1997; Sadofsky et al. 2008; Wade et al. 2006), Mexico (Cervantes and Wallace 2003; Johnson et al. 2009), Cascades (Ruscitto et al. 2010), Marianas (Shaw et al. 2008), Kamchatka (Auer et al. 2009; Portnyagin et al. 2007), Indonesia (Sisson and Bronto 1998), Aleutians (Zimmer et al. 2010) and Vanuatu (Métrich and Deloule 2014). Halogen concentrations in MORB are given for comparison

unusually high Cl/H<sub>2</sub>O ratios, such as those from Irazú (up to 0.48) (Benjamin et al. 2007) and Galunggung, western Java, Indonesia (0.25–0.53) (Sisson and Bronto 1998), are explained as having contribution from a highly saline fluid or melt. However, recent work has shown that water can be lost or gained in olivine-hosted melt inclusions via proton diffusion through the host crystal (e.g., Bucholz et al. 2013; Gaetani et al. 2012; Portnyagin et al. 2008). Halogen/H<sub>2</sub>O ratios determined from melt inclusions are valid *only* if water content is unmodified, thus correlations between water and halogen species should be treated with extreme caution (Bucholz et al. 2013). In addition to water loss via proton diffusion, the initial halogen/H<sub>2</sub>O ratios of melt inclusions may be complicated due to halogen fractionation from H<sub>2</sub>O during devolatilization of the subducting slab or during transport of slab-derived fluids through the mantle wedge (Wallace 2005) or late-stage magma interaction with brine (Métrich and Deloule 2014).

#### 8.4 Consequences for Evolution of the Mantle—Evidence of a Subducted Component

Because of their high fluid affinity, halogens strongly partition into subduction-zone fluids. As a result, halogens are generally predicted to be removed from the slab by devolatilization reactions prior to reaching subarc depths. However, increasing evidence shows that halogens can survive past the volcanic arc front.

### **8.4.1 Halogen Concentrations in the Depleted Upper Mantle (DMM) and Mid-Ocean Ridge Basalts (MORB)**

The concentration of Cl in the upper mantle (depleted MORB mantle, DMM) is estimated to range between 3 and 10  $\mu\text{g/g}$  (Burgess et al. 2002; Jambon et al. 1995; Lassiter et al. 2002; Schilling et al. 1980). However, others suggest Cl concentrations in the DMM as low as 0.4–1  $\mu\text{g/g}$  (Saal et al. 2002; Salters and Stracke 2004; Workman and Hart 2005; Frezzotti and Ferrando 2018; Klemme and Stalder 2018). Most MORB glasses contain  $\sim 20\text{--}50$   $\mu\text{g/g}$  Cl (Jambon et al. 1995; Michael and Schilling 1989; Schilling et al. 1980). Estimates of F concentrations in the DMM and MORB range from 11 to 65  $\mu\text{g/g}$  (Salters and Stracke 2004; Schilling et al. 1980) and from 16 to 109  $\mu\text{g/g}$  (Saal et al. 2002; Schilling et al. 1980), respectively. Bromine concentrations in the DMM range from 8 to 20  $\text{ng/g}$  (Burgess et al. 2002; Jambon et al. 1995; Schilling et al. 1980) and 100 to 200  $\text{ng/g}$  for MORB (Jambon et al. 1995; Schilling et al. 1980). Iodine concentrations in the DMM are estimated between 0.4 to 0.8  $\text{ng/g}$  (Burgess et al. 2002; Deruelle et al. 1992). MORB glasses average 8  $\text{ng/g}$  I (Deruelle et al. 1992). MORB F/Cl, Br/Cl and I/Cl ratios are  $\sim 1\text{--}10$ ,  $2.2\text{--}3.4 \times 10^{-3}$ , and  $3\text{--}9 \times 10^{-5}$ , respectively (Kendrick et al. 2012a, 2014b) (Fig. 8.1).

### **8.4.2 Halogens in Back-Arc Basin Basalts (BABB)**

BABB are enriched in halogens compared to MORB (Fig. 8.7). Manus Basin (Papua New Guinea) and Valu Fa Ridge (Lau Basin, Tonga Arc) basalt glasses have particularly high Cl concentrations (Kendrick et al. 2012b, 2014a; Kent et al. 2002; Sun et al. 2007). Sun et al. (2007) estimate that  $\sim 80\%$  of the Cl in Manus glasses are derived from slab fluids. However, the Cl enrichment is too great to be explained by Cl released from amphibole, phlogopite, or apatite (Kent et al. 2002). High I/Cl ratios (10 times the MORB value) in BABB glasses from the Manus Basin and the Valu Fa Ridge imply halogen contribution from serpentinite-derived fluids. MORB-like I/Cl and Br/Cl ratios in other BABB glasses (Woodlark Basin, North Fiji Basin, Fonualei Spreading Center (Lau Basin)) suggest a halogen contribution from the AOC (Kendrick et al. 2014a) (Fig. 8.1).

### **8.4.3 Halogens in Ocean Island Basalts (OIB)**

One way Cl recycling into the deeper mantle has been assessed is on the basis of Cl/K ratios in OIB. Chlorine has a similar compatibility to K during magmatic processes (Michael and Cornell 1998). Therefore, Cl/K ratios of uncontaminated basalts reflect assimilation of crustal material in the mantle source (e.g., Stroncik

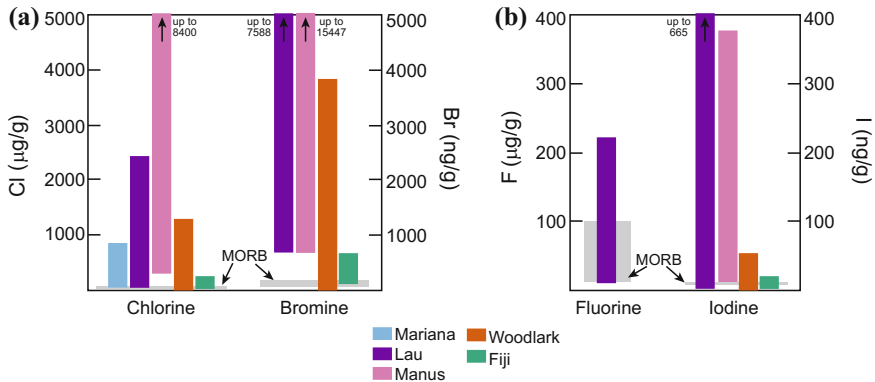


**Fig. 8.7** **a** Chlorine and Br concentrations and **b** F and I concentrations in back-arc basalt glasses from various back-arc basins. Halogen concentrations in MORB are given for comparison. Data from Bézous et al. (2009), Kendrick et al. (2014a), Kent et al. (2002), Stolper and Newman (1994) and Sun et al. (2007)

and Haase 2004). Normal MORB has Cl/K ratios as low as 0.01, whereas enriched MORB has Cl/K ratios of 0.05–0.08. Cl/K ratios >0.08 are due to either seawater alteration or assimilation of hydrothermally altered crustal material (Michael and Cornell 1998). Correlations between Cl/K ratios and radiogenic isotope ratios ( $^{87}\text{Sr}/^{86}\text{Sr}$  and  $^{206}\text{Pb}/^{204}\text{Pb}$ ) in OIB glasses and EM-type lavas are interpreted to reflect recycling of crustal material into OIB sources (Stroncik and Haase 2004; Workman et al. 2006) (Fig. 8.8b). The Cl isotope composition of OIB glasses also show trends with Cl/K ratios. For example, HIMU samples have a positive correlation between  $\delta^{37}\text{Cl}$  values and Cl/K, whereas enriched MORB samples have high  $\delta^{37}\text{Cl}$  values and low Cl/K ratios. This provides additional evidence for the survival of Cl into the upper mantle (John et al. 2010) (Fig. 8.8c). However, HIMU-type lavas from the Austral Islands have a relatively low Cl/K ratio of  $\sim 0.04$ , which is interpreted to reflect the effective removal of Cl during subduction and minimal recycling of Cl into the mantle via crustal residues (Lassiter et al. 2002). Discrepancies in the interpretation of Cl/K ratios in OIB basalts are partially due to uncertainty in the accepted value for the mantle K concentration (J. C. Lassiter, pers. comm.). Instead, Cl/Nb ratios may be a more effective tracer of Cl mobility (Sun et al. 2007).

As with BABB glasses, recent studies have used F, Cl, Br, and I concentrations in OIB glasses to assess halogen cycling into the deeper mantle (Kendrick et al. 2012b, 2014b). Cl/K, Br/K, and I/K in OIB glasses are all low and show correlations with  $^{87}\text{Sr}/^{86}\text{Sr}$  suggesting the presence of a subducted component. Interestingly, F/Nd does not correlate with  $^{87}\text{Sr}/^{86}\text{Sr}$  (this is also noted in basalt glasses from Samoa (Workman et al. 2006)), suggesting preferential subduction of F compared to the other halogens (Kendrick et al. 2014b).

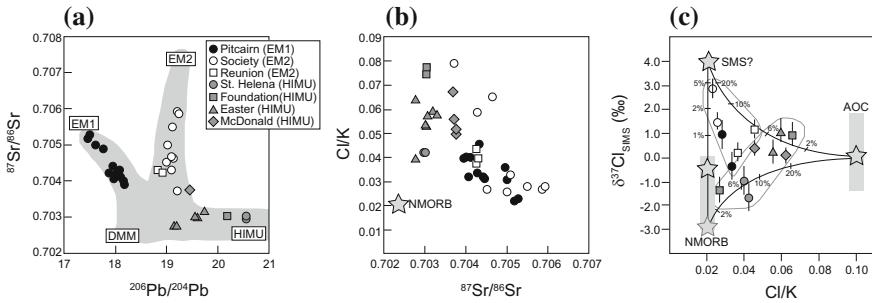


**Fig. 8.8** **a**  $^{206}\text{Pb}/^{204}\text{Pb}$  and  $^{87}\text{Sr}/^{86}\text{Sr}$  source characteristics of OIB glasses used in the halogen studies of John et al. (2010), Kendrick et al. (2014b) and Stroncik and Hasse (2004). Light gray area highlights mantle end members (Hofmann 2003). **b** Strong correlation between Cl/K ratios and Sr isotope ratios supports recycling of crustal material in OIB sources. Br/K and I/K ratios (not shown) show nearly identical trends with  $^{87}\text{Sr}/^{86}\text{Sr}$  as Cl/K. F/Nd shows no correlation with  $^{87}\text{Sr}/^{86}\text{Sr}$  (not shown). Data from Stroncik and Hasse (2004) and Kendrick et al. (2014b). **c**  $\delta^{37}\text{Cl}$  values (determined by SIMS) versus Cl/K ratios of OIB glasses (modified from John et al. 2010). EM1 and EM2 samples tend to have low Cl/K ratios and high  $\delta^{37}\text{Cl}$  values, whereas, HIMU samples have higher Cl/K ratios and lower  $\delta^{37}\text{Cl}$  values. AOC has a range of  $\delta^{37}\text{Cl}$  values from  $-1.4$  to  $+1.8\text{‰}$  (averaging  $\sim 0\text{‰}$ ), overlapping well with the range observed in HIMU glasses (Barnes and Cisneros 2012). The  $\delta^{37}\text{Cl}$  value of the upper mantle has not been agreed upon and ranges from  $-0.2$  to  $-3\text{‰}$  (Bonifacie et al. 2008b; Layne et al. 2009; Sharp et al. 2007, 2013). We prefer the value of  $-0.2\text{‰}$  (Sharp et al. 2007, 2013), but note that modelling presented in this figure (John et al. 2010) uses the extreme end member of  $-3\text{‰}$  (Layne et al. 2009). SMS is the hypothetical end member of deeply subducted sediments proposed by John et al. (2010), but not documented in other studies (e.g., Selverstone and Sharp 2013, 2015). (More details on Cl stable isotopes are presented in Sect. 8.7.1.)

## 8.5 Mass Budget Calculations

A summary of halogen inputs and outputs is presented in Figs. 8.9 and 8.10. The halogen budget of the global subduction system remains highly uncertain, chiefly because the only output at convergent margins that currently is reasonably well characterized is that from arc volcanoes. However, as with  $\text{H}_2\text{O}$ ,  $\text{CO}_2$  and other volatiles (e.g., Kelemen and Manning 2015), additional output pathways are likely but are extremely difficult to quantify. For example, contributions from the fore-arc, including geothermal systems, may be substantial, yet are poorly known. Magma ponding beneath or within the crust will lead to the generation and migration of a halogen-bearing fluid phase. While the fate of these halogens remains largely unknown, the participation of halogen-rich, magma-derived fluids in metamorphism and ore generation attests to the importance of this process. In addition, the contribution of crustal material eroded from the upper plate via mechanical coupling (e.g., Clift and Vannucchi 2004; Scholl and von Huene 2007) is not included in the halogen input estimates. Future work is necessary to achieve a robust halogen mass balance in convergent margins. Nevertheless, it is possible to evaluate preliminary constraints from the sources and sinks that can currently be estimated.

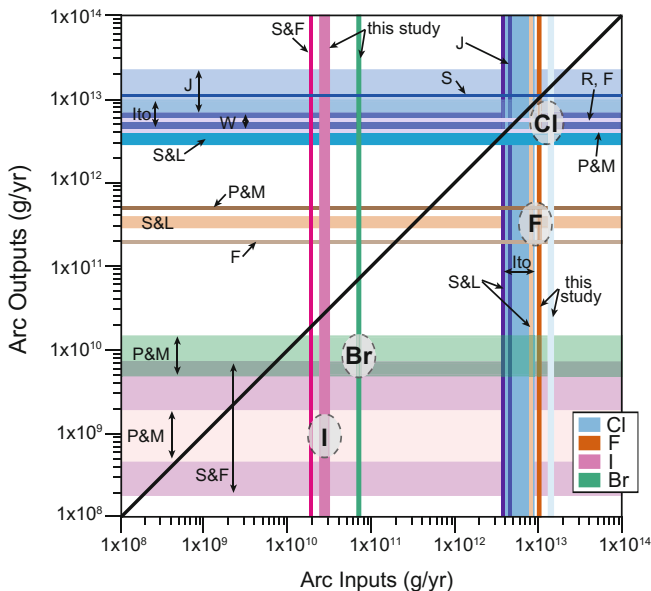


**Fig. 8.9** Halogen mass balance through the volcanic arc front. Chlorine fluxes are shown in shades of *blue*, F in shades of *orange-brown*, I in shades of *pink*, and Br in shades of *green*. *Gray ovals* enclose areas of input and output overlap with selected inputs from estimates that include halogen concentrations in serpentinites. Chlorine is the only halogen that is nearly in balance through the arc front, with some Cl likely returned to the mantle and some unaccounted for fraction lost beneath the fore-arc. Fluorine is returned to the mantle in greater proportion than Cl. Bromine and I have significant losses before the arc front that are unaccounted for in these calculations. *S&L* (Straub and Layne 2003), *J* (Jarrard 2003), *Ito* (Ito et al. 1983), *W* (Wallace 2005), *F* (Fischer 2008), *R* (Ruscitto et al. 2012), *P&M* (Pyle and Mather 2009), *S&F* (Snyder and Fehn 2002), *S* (Shinohara 2013)

### 8.5.1 Chlorine Flux Through Subduction Zones

Early mass balance calculations implied that the global Cl budget is nearly balanced, with Cl almost entirely returned to the Earth’s surface (Ito et al. 1983; Jarrard 2003; Ruscitto et al. 2012; Straub and Layne 2003). However, these studies did not include serpentinites in the calculations. Serpentinites are now known to be a major Cl host (e.g., Barnes and Sharp 2006; Kendrick et al. 2011; Scambelluri et al. 2004) and stable to great depths (up to 200 km) in subduction zones (Ulmer and Trommsdorff 1995; see Sect. 8.2.4). More recent calculations that include serpentinites suggest that Cl inputs may exceed outputs at subduction zones, thus allowing Cl to be recycled back into the mantle (Barnes and Straub 2010; John et al. 2011). Updated calculations (this contribution) also support the survival of Cl past the arc front (Table 8.1; Fig. 8.9). This conclusion is consistent with observations of saline fluid inclusions found in eclogitic terranes in the Alps (Philippot et al. 1998; Philippot and Selverstone 1991; Scambelluri et al. 1997; Selverstone et al. 1992);

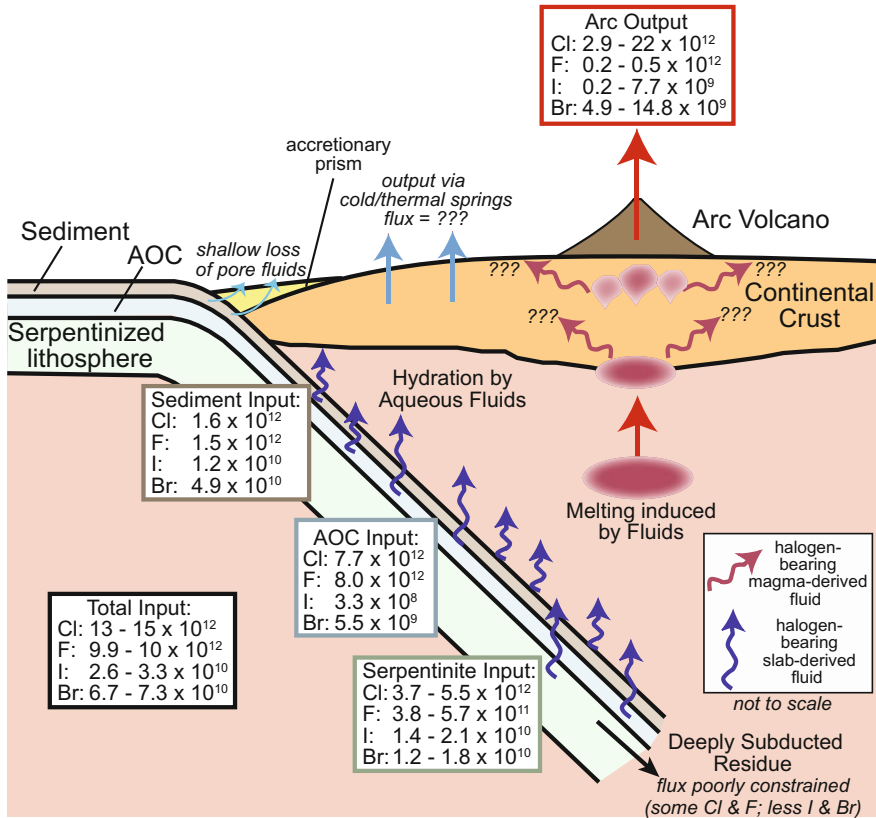


**Fig. 8.10** Schematic diagram illustrating halogen fluxes through the subduction zone. Arc output flux values are from references given in Table 8.1. Influx calculations are from this contribution. Pore fluids are assumed to be lost at very shallow depths (by  $\sim 5$  km) and are therefore ignored in the calculations. The unknown extent of serpentinization of the subducting oceanic lithosphere leads to uncertainties in the serpentinite halogen input. Halogen loss via progressive metamorphic dehydration reactions of sediments, altered oceanic crust, and serpentinites is poorly constrained leading to uncertainties in the halogen content in the residual slab. Despite these uncertainties, there is clear evidence for the return of halogen from surficial reservoirs into the upper mantle

high Cl concentrations retained in high-pressure dehydrated residues of serpentinites (John et al. 2011; Kendrick et al. 2011; Scambelluri et al. 2004); and high concentrations of Cl in back-arc glasses (Bézos et al. 2009; Kendrick et al. 2014a; Kent et al. 2002; Stolper and Newman 1994; Sun et al. 2007). There is also evidence for deep Cl recycling into the upper mantle by Cl/K, Br/Cl, and I/Cl ratios and  $\delta^{37}\text{Cl}$  values measured in plume-related basalts (John et al. 2010; Kendrick et al. 2014b; Stroncik and Haase 2004; Workman et al. 2006). Based on halogen concentrations in OIB, BABB, and MORB glasses, up to 10% of the total subducted Cl may survive into the upper mantle (Kendrick et al. 2014b).

### 8.5.2 *Fluorine Flux Through Subduction Zones*

Mass balance calculations overwhelmingly suggest that F is efficiently returned to the mantle (Table 8.1; Fig. 8.9). These calculations are supported by F concentrations in BABB and OIB glasses and arc front melt inclusions, which suggest that F is decoupled from Cl during the subduction process and preferentially returned to the mantle (Kendrick et al. 2014b; Straub and Layne 2003). Kendrick et al. (2014b) speculate that the preferential subduction of F versus Cl may be due to the higher solubility of F in nominally anhydrous minerals produced during subduction-driven dehydration (Bernini et al. 2013; Beyer et al. 2012; Dalou et al. 2012; Fabbriozio et al. 2013) and the higher compatibility of F in micas and amphiboles relative to Cl (e.g., Morrison 1991; Munoz 1984; Volfinger et al. 1985). Preferential retention of F in subducted lithologies may also be due to the sequestration of F in Ti-clinohumite (cf., Evans and Trommsdorff 1983; John et al. 2011). Future studies addressing F behavior in subduction zones should help address the decoupling of Cl and F.

### 8.5.3 *Iodine and Br Fluxes Through Subduction Zones*

Mass balance calculations show a greater input of Br and I into the subduction system than is returned to the surface via arc volcanism (Table 8.1; Fig. 8.9). Calculations by Snyder and Fehn (2002) estimate that up to 38% of the total subducted I may reach the volcanic arc front. I/Cl and Br/Cl ratios of OIB glasses suggest that <4–10% of the total subducted I and Br reaches the upper mantle (Kendrick et al. 2014b). Work on halogen concentrations in serpentinites demonstrates that I and Br are lost from serpentinites at shallower depths than either Cl or F (John et al. 2011; Kendrick et al. 2011, 2013). Loss of Br and I at depths shallower than the arc front is the likely explanation for the imbalance. Little work has been done on Br loss during subduction, but I shows dramatic losses at shallow depths. Marine sediments, the major iodine reservoir, lose 75–95% of their I by ~400 °C (Muramatsu and Wedepohl 1998). This estimate is supported by cosmogenic <sup>129</sup>I data of fore-arc fluids which imply mobilization of I from subducting sediments (Muramatsu et al. 2001; Tomaru et al. 2007) (see Sect. 8.7.2).

## 8.6 Halogens and Fluid Chemistry

High concentrations of halogens in subduction-zone fluids (estimated chlorine concentrations >1 wt% (Kent et al. 2002; Portnyagin et al. 2007; Stolper and Newman 1994; Straub and Layne 2003) and F concentrations up to ~1 wt% (Portnyagin et al. 2007)) have important consequences for the transport of metals and trace elements (Keppler 1996, 2017; Manning 2004; Webster 2004).

### 8.6.1 *Physical Properties and Solute Structure*

The addition of salts, such as NaCl and KCl, to H<sub>2</sub>O changes fluid physical properties and the solute structure relative to pure H<sub>2</sub>O. Recent experimental and theoretical studies at subduction-zone conditions (Mantegazzi et al. 2013; Sakuma and Ichiki 2015) show that at a given P and T, increasing salinity in NaCl-H<sub>2</sub>O solutions causes the sound speed in the fluid to decrease. This translates to increases in the fluid density at all subduction-zone pressures and temperatures. For example, at 800 °C and 3 GPa, the density of pure H<sub>2</sub>O is 1160 kg/m<sup>3</sup>. NaCl concentrations of 1 and 3 molal yield solution densities of 1250 and 1350 kg/m<sup>3</sup>, respectively, or 7 and 16% higher (Mantegazzi et al. 2013). As discussed below, salt solutions are strongly ionized at all subduction conditions. The increases in density with rising salt concentration arise from the volume reduction associated with ion solvation by H<sub>2</sub>O (Sakuma and Ichiki 2015). Mantegazzi et al. (2013) derived thermodynamic and transport properties from an equation of state based on their sound speed determinations. Results indicate that, as NaCl concentration rises from 0 to 3 molal at 800 °C and 3 GPa, thermal expansivity and isothermal compressibility decrease, whereas adiabatic compressibility increases. It is important to note that the inferred isobaric heat capacity does not change systematically with salinity and is highly discrepant with pure H<sub>2</sub>O at high pressure (Wagner and Pruß 2002).

### 8.6.2 *Effects on Phase Equilibria*

The addition of salts to metamorphic H<sub>2</sub>O has a very different effect on phase equilibria than addition of CO<sub>2</sub> and other non-polar gases (Manning and Aranovich 2014). This is because in mixtures of NaCl and H<sub>2</sub>O, the H<sub>2</sub>O activity displays negative departures from ideality at high pressure and temperature (e.g., Aranovich and Newton 1996, 1997; Mantegazzi et al. 2013; Shmulovich and Graham 1996; Tropper and Manning 2004), whereas CO<sub>2</sub>-H<sub>2</sub>O mixtures show comparatively larger, and positive, departures from ideality (Aranovich and Newton 1999; Halbach and Chatterjee 1982; Holloway 1977; Kerrick and Jacobs 1981; Saxena and Fei 1987). Although studies of mixing properties of metamorphic fluids typically focus on pressures lower than those attained during subduction, limited investigations at high pressure (e.g., Mantegazzi et al. 2013; Tropper and Manning 2004) confirm the conclusions above.

The contrasting properties of mixing H<sub>2</sub>O with salts (e.g., NaCl, KCl) versus CO<sub>2</sub> and other non-polar gases have several important petrologic consequences (Manning and Aranovich 2014; Mantegazzi et al. 2013). The first is that, at a given pressure and concentration of salt or CO<sub>2</sub>, the melting temperature of the coexisting mineral assemblage will be higher in the presence of the salt solution. Aranovich et al. (2013) showed that at 1 GPa and in the presence of a (Na,K)Cl solution with an H<sub>2</sub>O mole fraction of 0.7, the haplogranite melting temperature is 100 °C higher

than when coexisting with an H<sub>2</sub>O-CO<sub>2</sub> fluid of the same H<sub>2</sub>O mole fraction. Their experimental results suggest that the disparity should increase at higher pressures. Thus, high-salinity aqueous solutions can be expected to suppress the onset of slab melting relative to pure H<sub>2</sub>O or H<sub>2</sub>O-CO<sub>2</sub>. Second, dehydration reactions involving key hydrous minerals will proceed at lower temperatures (i.e., generally shallower depths) than would be the case in the presence of pure H<sub>2</sub>O or H<sub>2</sub>O-CO<sub>2</sub> mixtures. Finally, the different mixing properties lead to the persistence of a large miscibility gap at high concentrations of salt and CO<sub>2</sub> in the bulk fluid (e.g., Aranovich et al. 2010; Heinrich 2007; Liebscher 2010; Manning et al. 2013). At sufficiently high concentrations of CO<sub>2</sub> and salt, this can lead to the creation of two fluid phases, one of which is a brine with a high carrying capacity for metals derived from the slab.

### 8.6.3 Aqueous Geochemistry of Halogens

#### 8.6.3.1 Alkali-Chloride Solutions

The main rock-forming alkali metals are Na and K. The most abundant halogen is Cl. These elements will play major roles in governing the effects of halogens on fluid-mediated processes in subduction zones. Here we evaluate the effects of subduction-zone pressures and temperatures on these dissolved solutes. At any pressure and temperature, NaCl or KCl ion pairs in an aqueous solution (NaCl<sub>aq</sub>, KCl<sub>aq</sub>) will partly dissociate to their constituent ions



Polynuclear clusters (e.g., NaCl<sub>2</sub><sup>-</sup>, K<sub>2</sub>Cl<sup>+</sup>, NaKCl<sub>2</sub>) may be present at elevated salinity at low pressure and high temperature (Oelkers and Helgeson 1993); however, their concentrations are likely negligible at high-pressure subduction conditions (Sakuma and Ichiki 2015).

The extent of dissociation in Eq. 8.1 governs the availability of Cl<sup>-</sup> to interact with other metals in solution and is influenced by homogeneous equilibria among dissolved solutes. In an aqueous NaCl solution, these are

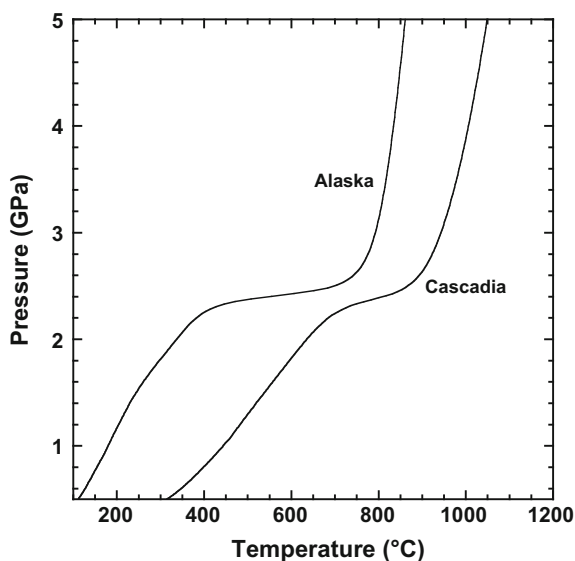


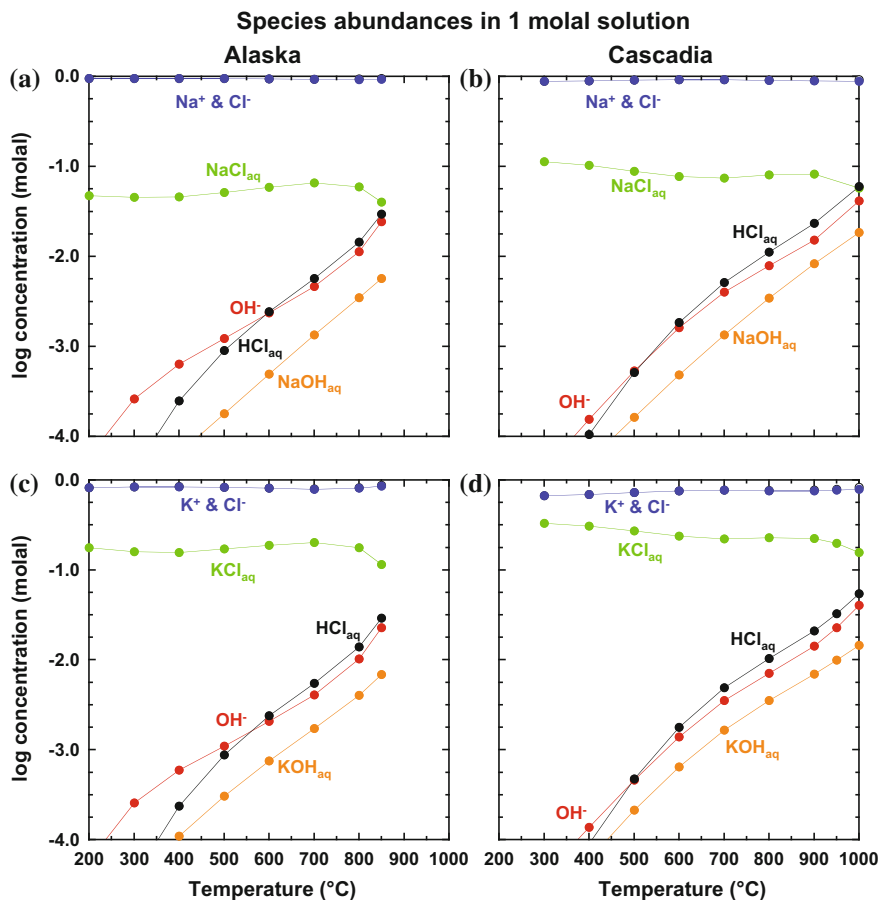
The distribution of species, pH and extent of dissociation can be determined for a given NaCl concentration by combining equilibrium constants for Eqs. 8.1–8.5, solute activity models, and the charge balance constraint. Taking the standard state of aqueous species to be the unit activity of the hypothetical 1 molal solution referenced to infinite dilution, species concentrations and activity coefficients were calculated using the Güntelberg equation for ion activities and assuming unit activity coefficients of neutral species (Manning 2013). Pressures and temperatures were taken from the thermal models of Syracuse et al. (2010) for Alaska and Cascadia slab-top sediments (D80 models, Fig. 8.11), corresponding respectively to relatively cool and warm subduction geotherms. The Deep Earth Water Model (v 11.0.1) of Sverjensky et al. (2014) was used to calculate equilibrium constants, as well as the density and dielectric constant of H<sub>2</sub>O for calculation of the solvent A parameter.

Figure 8.12 a shows the distribution of species in a 1 molal NaCl solution at the temperature of the Alaska sediment top. Note that pressure increases with temperature as well (Fig. 8.11). It can be seen that Na<sup>+</sup> and Cl<sup>-</sup> are the predominant species everywhere along this subduction geotherm. The concentrations of HCl<sub>aq</sub> and NaOH<sub>aq</sub> ion pairs increase with temperature and pressure but are always lower in abundance than Na<sup>+</sup> and Cl<sup>-</sup>. The rise in OH<sup>-</sup> concentration with temperature and pressure signals an increasingly alkaline pH (see below).

KCl has a greater tendency to form ion pairs than does NaCl. Comparison of Fig. 8.12a, b shows that, along the Alaskan sediment geotherm, KCl<sub>aq</sub>

**Fig. 8.11** Model subduction-zone geothermal gradients from Syracuse et al. (2010). P-T conditions correspond to the sediments at the slab top, using the D80 set of models in which thermomechanical coupling between the slab and mantle wedge begins at 80 km depth





**Fig. 8.12** Results of thermodynamic modeling of 1 molal NaCl and KCl solutions. Conditions correspond to model slab-top geotherms from Fig. 8.11, i.e., pressure and temperature co-vary. *Filled circles* represent conditions at which modeling was conducted. Equilibrium constants and solvent parameter A were calculated from the DEW model 11.0.1 (Sverjensky et al. 2014), to a maximum pressure of 6 GPa. Ion activities were computed using the Güntelberg equation. Neutral species were assumed to have a unit activity (Manning 2013). Activity coefficients and species concentrations were calculated using a modified version of the program EQBRM (Anderson and Crear 1993). For many lithologies, parts of both thermal models are likely metastable with respect to H<sub>2</sub>O-saturated melting

concentration is everywhere greater than that of NaCl<sub>aq</sub>. Concentrations of K<sup>+</sup> and Cl<sup>-</sup> are correspondingly slightly lower.

In general, the thermodynamic data indicate that higher temperatures, at a given depth, and lower pressures, at a given temperature, favor ion pair formation. The implication for subduction geotherms is that NaCl and KCl will be more associated along hotter subduction geotherms, such as that of the sediment top in the Cascadia

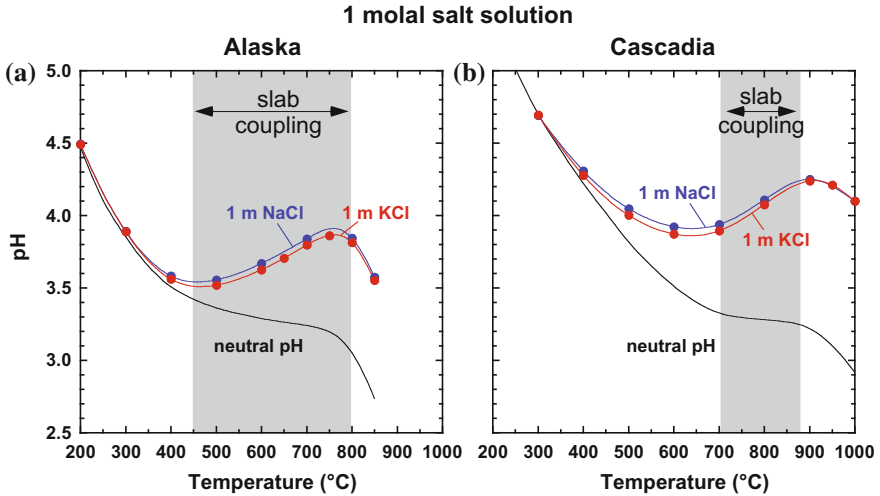


**Fig. 8.13** pH of fluids in thermodynamic models shown in Fig. 8.12. Neutral pH at high P and T is much lower than 7 due to a greater extent of dissociation of  $\text{H}_2\text{O}$  (e.g., Manning 2013). The pH of 1 molal NaCl and KCl solutions is always more alkaline than acid-base neutrality, and becomes increasingly so with depth in both subduction zones. This is due to the increasing stability of  $\text{HCl}_{\text{aq}}$  (see text). The temperature range of thermomechanical slab coupling is shown in the shaded regions (Syracuse et al. 2010)

subduction zone (Fig. 8.12c, d). It can be seen in Fig. 8.12 that the relative abundance of  $\text{NaCl}_{\text{aq}}$  and  $\text{KCl}_{\text{aq}}$  in 1 molal salt solutions is greater on the Cascadia path relative to the Alaska path, due to the lower pressure at each temperature in the former system (Fig. 8.11).

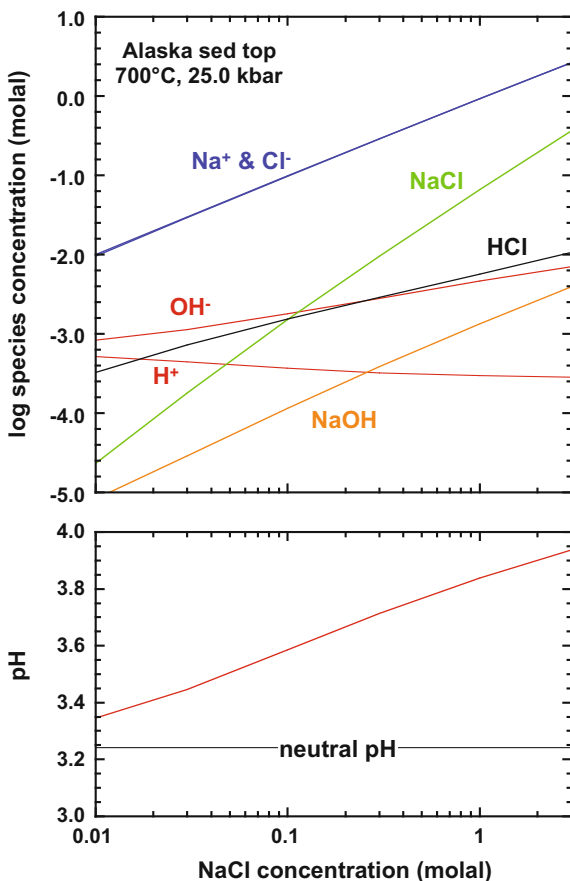
The pH of 1 molal salt solutions varies with temperature and depth along slab geotherms (Fig. 8.13). Neutral pH, as determined by the equilibrium constant for Eq. 8.5, decreases from 7 at ambient conditions to less than 4 at moderate temperature and high pressure of the sediment top along the Alaskan and Cascadian geotherms. This indicates that, at subduction zone conditions,  $\text{H}_2\text{O}$  exhibits a much stronger propensity to ionize relative to shallow crustal conditions. The concentration of  $\text{HCl}_{\text{aq}}$  is always greater than that of  $\text{NaOH}_{\text{aq}}$  (Fig. 8.12). Therefore, the pH of 1 molal NaCl or KCl solution is everywhere alkaline due to the greater concentration of  $\text{Na}^+$  or  $\text{K}^+$  than  $\text{Cl}^-$ . The two salts exhibit similar pH changes along slab geotherms, though it can be seen that KCl yields slightly less alkaline conditions than does NaCl due to the greater association of the former salt (Fig. 8.12). All else being equal, the more dissociated the salt, the more alkaline the solution.

At low temperatures where  $\text{HCl}_{\text{aq}}$  concentration is very low, the pH differs negligibly from neutrality. However, as temperature increases with depth along subduction paths, the growing concentration of  $\text{HCl}_{\text{aq}}$  ion pairs drives the solution to progressively more alkaline pH. Notably, where the slab and overriding mantle

begin to couple mechanically, the resultant nearly isobaric temperature increase leads to greater  $\text{HCl}_{\text{aq}}$  formation relative to  $\text{NaOH}_{\text{aq}}$  or  $\text{KOH}_{\text{aq}}$ , resulting in a significant increase in alkalinity in this region of the subduction zone. Maximum departure from neutral pH is predicted at the deepest, highest temperature conditions. At these conditions, a 1 molal salt solution would have pH  $\sim 0.8$  and  $\sim 1.2$  units greater than the acid-base neutrality at the most extreme Alaskan and Cascade sediment top conditions calculated.

The relationships portrayed in Figs. 8.12 and 8.13 depend on salt concentration. This is illustrated in Fig. 8.14, which shows the variation in calculated species abundance as a function of total NaCl concentration at 700 °C and 2.5 GPa, along the Alaskan sediment top. The solution is always dominated by ionic species. However, the relative abundance of the ion pairs controls the pH, regardless of concentration. As the  $\text{HCl}_{\text{aq}}$  concentration rises, the pH is forced to increase as  $\text{H}^+$  is consumed relative to  $\text{OH}^-$ .

**Fig. 8.14** Variation in species abundance with NaCl concentration at Alaskan slab-top conditions of 700 °C, 2.5 GPa. Variations in equilibrium constants with P and T lead to small differences between  $\text{Na}^+$  and  $\text{Cl}^-$  concentration that are unresolvable at the scale of plotting. Compensating variations in  $\text{OH}^-$  and  $\text{H}^+$  yield charge balance and changing pH with NaCl. All model parameters as in Fig. 8.12



### 8.6.3.2 Role of Saline Fluids in Metal Transport

It is well known that halogen-rich fluids are responsible for significant metal transport and deposition in shallow crustal environments, such as hydrothermal ore deposits. In general, metal- $\text{Cl}^-$  and  $\text{F}^-$  complex stability are not strongly pressure dependent. Halogen complexing can therefore be expected to play an important role in metal mobility in subduction-zone environments.

Kepler (1996) showed that trace-element partitioning between clinopyroxene and a 5 m (NaK)Cl solution indicate higher solubility of Rb, Ba, U, K, Pb, and Sr relative to pure  $\text{H}_2\text{O}$ , and that fluid-clinopyroxene partition coefficients yield trace-element patterns (relative to NMORB) that are similar to subduction-zone volcanics. He concluded that  $\text{Cl}^-$  fluids could be responsible for trace element transport in subduction zones.

The thermodynamic basis for this behavior is the relative stability of metal-halogen complexes in the aqueous phase. For example, divalent metal  $\text{M}^{+2}$  and  $\text{Cl}^-$  will form  $\text{Cl}^-$  complexes via the stepwise association reactions



A generic hydrolysis reaction for the oxide of metal M can be written as



It is evident that formation of  $\text{MCl}^+$  and  $\text{MCl}_{2\text{aq}}$  complexes requires forward progress of reaction Eq. (8.7). Thus, more positive equilibrium constants for reactions Eqs. (8.6) and (8.8) indicate an increase in the transport susceptibility of a particular metal by  $\text{Cl}^-$  complexes.

Figure 8.15 compares equilibrium constants for the first association reaction (8.5) for a range of divalent metals along the Alaskan and Cascadian slab-top P-T paths (Fig. 8.11). Equilibrium constants for reactions involving alkaline earth and transition metals increase with temperature (and depth) along both paths. The equilibrium constants are broadly similar regardless of the path, indicating relatively little dependence on pressure. Of the alkaline earths, values of  $\log K$  for Mg, Sr, and Ba  $\text{Cl}^-$  complex formation are very similar, but values for Ca are higher. Regardless of the temperature of the path, Ca will be more strongly mobilized and redistributed by  $\text{Cl}^-$ -bearing fluids. Of the transition metals for which data are available, Zn, Mn, and Pb display a stronger tendency to form  $\text{Cl}^-$  complexes than do the alkaline earth metals. It can be expected that these elements are strongly mobilized by  $\text{Cl}^-$  solutions in subduction-zone settings. This simple analysis shows that, with the recent publication of robust thermodynamic models for high pressure fluids (Sverjensky et al. 2014), it will soon be possible to attempt more quantitative analyses of the role of alkali halides on metal cycling in subduction zones.

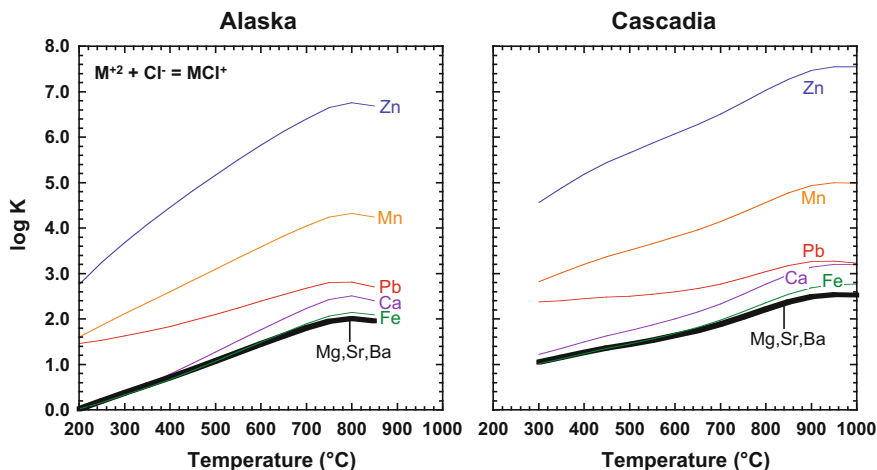


**Fig. 8.15** Logarithms of equilibrium constants for the first association reaction involving divalent metal (M) chlorides. Data from the DEW model 11.0.1 (Sverjensky et al. 2014)

## 8.7 Halogen Isotopes

In the last  $\sim 15$  years, stable Cl isotopes ( $^{35}\text{Cl}$  and  $^{37}\text{Cl}$ ) and cosmogenic halogen isotopes ( $^{36}\text{Cl}$  and  $^{129}\text{I}$ ) have been used to trace volatile sources through subduction zones. Studies employing Br stable isotopes ( $^{79}\text{Br}$  and  $^{81}\text{Br}$ ; Aston 1920) are limited and to date no published work has used Br isotopes as tracers in subduction zones.

### 8.7.1 Stable Cl Isotopes ( $^{35}\text{Cl}$ and $^{37}\text{Cl}$ )

Chlorine has two stable isotopes,  $^{35}\text{Cl}$  and  $^{37}\text{Cl}$ , with relative abundances of 75.77% and 24.23%, respectively. Chlorine isotope ratios are reported in standard per mil notation ( $\delta^{37}\text{Cl}$ ) relative to Standard Mean Ocean Chloride (SMOC), which is defined to be 0‰ (Kaufmann et al. 1984). In the last 20 years, much work has focused on defining the Cl isotope composition of various Cl reservoirs (Fig. 8.16).

The Cl isotope composition of the upper mantle has been a subject of debate in recent years. Sharp et al. (2007) proposed a relatively homogeneous MORB mantle  $\delta^{37}\text{Cl}$  value of  $-0.2 \pm 0.5\%$ . Bonifacie et al. (2008b) argued that the mantle has a value of  $\leq -1.6\%$ , based on the observation of lower  $\delta^{37}\text{Cl}$  values in samples with lower Cl concentration. However, these low  $\delta^{37}\text{Cl}$  values may not reflect uncontaminated samples, but rather analytical error associated with the analysis of small samples (Sharp et al. 2013). Layne et al. (2009) proposed a  $\delta^{37}\text{Cl}$  value of  $-3.0\%$  based on SIMS measurements of two MORB samples. Recently, using new analyses of mantle and chondritic material, Sharp et al. (2013) convincingly argued

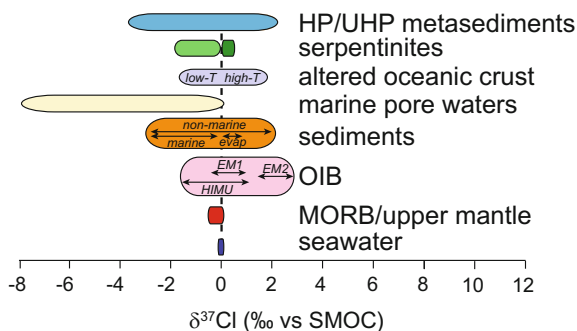


**Fig. 8.16**  $\delta^{37}\text{Cl}$  values of various crustal and mantle reservoirs.  $\delta^{37}\text{Cl}$  values from Arcuri and Brimhall (2003), Barnes and Cisneros (2012), Barnes et al. (2006, 2008, 2009a, b), Barnes and Sharp (2006), Bonifacie et al. (2007b), Boschi et al. (2013), Godon et al. (2004), John et al. (2010), Ransom et al. (1995), Selverstone and Sharp (2013, 2015), Sharp et al. (2007, 2013) and Spivack et al. (2002)

for a mantle value of  $-0.2 \pm 0.3\text{‰}$ , analytically indistinguishable from a chondrite value of  $-0.3 \pm 0.3\text{‰}$ . However, the mantle likely preserves some heterogeneities due to the subduction of crustal material (John et al. 2010; Sharp et al. 2007).

Seawater, brines, and evaporites have average  $\delta^{37}\text{Cl}$  values of  $0.0 \pm 0.5\text{‰}$  with minimal change through geologic time (e.g., Eastoe et al. 1999, 2007; Eastoe and Peryt 1999; Eggenkamp et al. 1995; Kaufmann et al. 1984). Marine sedimentary pore fluids are negative, down to  $-7.8\text{‰}$  (Bonifacie et al. 2007b; Godon et al. 2004; Ransom et al. 1995; Spivack et al. 2002). Marine and non-marine sedimentary material has  $\delta^{37}\text{Cl}$  values ranging from  $-3.0\text{‰}$  to  $+2.0\text{‰}$  ( $n = 82$ ) with most non-evaporite marine samples having values between  $\sim -2\text{‰}$  and  $0\text{‰}$  (Arcuri and Brimhall 2003; Barnes et al. 2008, 2009b; Selverstone and Sharp 2015). AOC has  $\delta^{37}\text{Cl}$  values ranging from  $-1.6$  to  $+1.8\text{‰}$  (Barnes and Cisneros 2012; Bonifacie et al. 2007a). Negative values are dominantly from low-temperature altered, clay-bearing AOC. High-temperature altered, amphibole-bearing AOC is isotopically positive (Barnes and Cisneros 2012). Most seafloor serpentinization results from interaction with seawater producing serpentinites with  $\delta^{37}\text{Cl}$  values between  $\sim 0.0$  and  $+0.5\text{‰}$  (Barnes et al. 2009a; Barnes and Sharp 2006; Boschi et al. 2013). However, serpentinites can interact with isotopically negative pore fluids, producing rare isotopically negative serpentinites (Barnes et al. 2006; Barnes and Sharp 2006).

The role of subduction metamorphism on the modification of the Cl isotope composition of high-pressure, subducted material is an area of current research. Theoretical calculations predict that little to no Cl isotope fractionation should occur at elevated temperatures (Schauble et al. 2003) and  $\delta^{37}\text{Cl}$  values are thus expected to remain unaltered during metamorphic devolatilization and Cl loss. Work on high-pressure serpentinites and deserpentinized peridotites from the Alps confirm that no significant Cl isotope fractionation occurs during dehydration of the serpentinites (John et al. 2011; Selverstone and Sharp 2013). However, Selverstone

and Sharp (2013) showed that the  $\delta^{37}\text{Cl}$  values of serpentinites can be modified at lower pressures during exhumation following subduction. High-pressure and ultra high-pressure sedimentary rocks have  $\delta^{37}\text{Cl}$  values ranging from  $-3.7$  to  $+2.2\%$  ( $n = 33$ ) (John et al. 2010; Selverstone and Sharp 2013), in good agreement with data from unmetamorphosed sedimentary rocks ( $\delta^{37}\text{Cl} = -3.0$  to  $+1.7\%$ ) (Selverstone and Sharp 2015). John et al. (2010) hypothesize that deeply subducted sediments may be characterized by high  $\delta^{37}\text{Cl}$  values, possibly up to  $+4\%$ , but other studies have yet to document such elevated values.

A study of metasomatized, suprasubduction-zone mantle preserved in the Finero complex in the Alps documented two distinct fluid infiltration events characterized by two different  $\delta^{37}\text{Cl}$  values (Selverstone and Sharp 2011). One fluid endmember had  $\delta^{37}\text{Cl} \leq -2\%$ , was associated with low  $\delta\text{D}$ , had high O-fugacity, and had elevated Si, Al, and Ca contents. This fluid produced amphibole-rich segregations in the peridotites. The other fluid had  $\delta^{37}\text{Cl}$  values  $\geq +2\%$ ; high  $\delta\text{D}$  and  $\delta^{18}\text{O}$  values; and high alkali, HFSE, LILE, Cr, and Cl contents. This latter fluid resulted in pervasive growth of phlogopite in the peridotites.

Previous work employing Cl stable isotopes as a tracer of source in subduction zones has been limited to the Izu-Bonin-Mariana (IBM), and the Central and South America systems (Barnes et al. 2008, 2009b; Barnes and Straub 2010; Chiaradia et al. 2014).  $\delta^{37}\text{Cl}$  values of outputs from across the IBM system (fore-arc serpentinites, volcanic front ash, back-arc lavas) vary and were interpreted to imply fluid sources at different depths within the subduction zone (Barnes et al. 2008).<sup>4</sup> Volcanic front ash data show little variation in  $\delta^{37}\text{Cl}$  values along the length of the arc and indicate a fluid contribution from sediments and altered oceanic crust.  $\delta^{37}\text{Cl}$  values of outputs from both forearc seamounts and reararc cross-chains (chain of seamounts at high angles to the arc front) suggest a serpentinite-derived fluid source. Fluids released at shallow depths, due to the transition from chrysotile/lizardite to antigorite in subducting lithospheric serpentinite, contribute to forearc seamounts. In contrast, fluids released at  $\sim 200$  km depth from the breakdown of antigorite contribute to rear arc cross-chains (Barnes et al. 2008). Subsequent work focusing solely on 0–44 Ma tephra from the Izu-Bonin arc show no correlation between  $\delta^{37}\text{Cl}$  values and either  $^{207}\text{Pb}$  or Sr isotopes, which are controlled by fluids from subducting sediment and igneous crust, respectively. This lack of correlation was used as an argument for a serpentinite Cl reservoir (Barnes and Straub 2010).

In contrast to the IBM arc, ashes from the Central America volcanic front record large Cl isotope variations along the length of the arc ( $-2.6$  to  $+3.0\%$ ), consistent with different Cl sources (Barnes et al. 2009b). Nicaraguan ashes record interaction

---

<sup>4</sup>The Cl isotope composition of volcanic outputs has focused on lavas, tephra, and glasses. Volcanic gases can have unusually high  $\delta^{37}\text{Cl}$  values (up to  $+12\%$ ). Volcanoes with these high values are distinguished by high-T fumaroles ( $>100$  °C) and large volcanic lakes and/or hydrothermal systems. These high values are explained by kinetic fractionation in which  $^{35}\text{Cl}$ -enriched HCl preferentially dissolves in the aqueous condensate along the flow path producing a  $^{37}\text{Cl}$ -enriched HCl vapor (Sharp et al. 2010). As a consequence, volcanic gas samples, particularly those from high-T systems, are avoided for use as a tracer of source.

with sediment and/or serpentinite-derived fluids, whereas samples from the northern and southern ends of the arc reflect a more mantle-like signature, consistent with conclusions from other geochemical tracers, such as  $\delta^{15}\text{N}$ ,  $\delta^{18}\text{O}$ , and Ba/La (e.g., Patino et al. 2000; Fischer et al. 2002; Eiler et al. 2005).

Recent work on across arc Cl isotope variations in Ecuadorian lavas show that changes in  $\delta^{37}\text{Cl}$  values across the arc correlate well with slab fluid indices (e.g., Ba/La, Pb/Ce). The overall decrease in  $\delta^{37}\text{Cl}$  values away from the trench can be interpreted in the frame of previous petrogenetic models of Ecuadorian volcanoes. Here magmas are formed by a steadily decreasing melt fraction of the mantle induced by a steadily decreasing amount of fluids released by the subducted slab away from the trench (Chiaradia et al. 2014).

### 8.7.2 *Cosmogenic Halogen Isotopes ( $^{36}\text{Cl}$ and $^{129}\text{I}$ )*

Iodine has one stable isotope ( $^{127}\text{I}$ ) and one long-lived isotope ( $^{129}\text{I}$ ).  $^{129}\text{I}$  is a cosmogenic nuclide with a half-life of 15.7 Myr, allowing for age determinations up to 80 Ma.  $^{129}\text{I}$  forms either from interaction with cosmic rays with Xe isotopes in the atmosphere or by the spontaneous fission of  $^{238}\text{U}$  in the crust (Fabryka-Martin et al. 1985). Anthropogenic  $^{129}\text{I}$  is also produced as a byproduct of nuclear weapons testing and nuclear fuel reprocessing (e.g., Muramatsu and Ohmomo 1986). Due to the high concentration of I in marine sediments and pore fluids, most studies use  $^{129}\text{I}$  as a tracer of sediment and/or sedimentary pore fluid recycling through the fore-arc (e.g., Fehn and Snyder 2003; Fehn et al. 2007; Muramatsu et al. 2001; Tomaru et al. 2007). Previous work on I cycling through the oceans has pointed out a large I imbalance in the marine cycle. There is a large flux of iodine from marine organic material into sediments. In addition, the oceans lose I to the atmosphere in the form of iodinated hydrocarbons. Flux of I from river input into the ocean cannot balance ocean I loss (Muramatsu et al. 2001; Muramatsu and Wedepohl 1998). However, the release of I from subducting sediments into fore-arc fluids and ultimately back into the oceans may address this imbalance (Muramatsu et al. 2001). Many I-enriched brines and fluids are documented within the forearc of Japan and New Zealand (e.g., Fehn and Snyder 2003; Fehn et al. 2007; Muramatsu et al. 2001; Tomaru et al. 2007), as well as in the continental slope of Peru (Martin et al. 1993). In New Zealand,  $^{129}\text{I}/\text{I}$  ratios suggest an old I source to the fore-arc fluids, possibly sourced from the accretionary wedge and not derived from actively subducting sediments (Fehn and Snyder 2003; Fehn et al. 2007). However, in several localities in Japan,  $^{129}\text{I}$  data support I sourced from subducting marine sediments and not by derivation from accretionary host rock (Muramatsu et al. 2001; Tomaru et al. 2007). Their similar geochemistry with respect to other fore-arc brines has led others to suggest that these Japanese fore-arc fluids may in fact be derived from the upper plate (Fehn 2012).

A few studies have used  $^{129}\text{I}$  to address sediment recycling at or near the arc volcanic front (e.g., Fehn et al. 2002; Snyder and Fehn 2002).  $^{129}\text{I}/\text{I}$  ratios in fluids

from hydrothermal springs, crater lakes, and fumaroles from the Central American arc front suggest I is predominantly sourced from subducting sediments and diluted by groundwater or modified by older crustal I (Snyder and Fehn 2002).  $^{129}\text{I}/\text{I}$  ratios from crater lakes from White Island, New Zealand and Copahue, Argentina also support the derivation of I from subducted sediments (Fehn et al. 2002). Although data is limited,  $^{129}\text{I}$  indicates a subducted marine sedimentary source for all arc volcanic fluids studied (Fehn 2012).

In addition to the two Cl stable isotopes discussed in Sect. 8.7.1, Cl has one long-lived isotope ( $^{36}\text{Cl}$ ) with a half-life of 0.301 Myr.  $^{36}\text{Cl}$  is produced by the interaction of cosmic rays with Ar isotopes in the atmosphere and by cosmic ray interaction with stable Cl, Ca, and K in the crust. Like  $^{129}\text{I}$ ,  $^{36}\text{Cl}$  is also produced anthropogenically as a waste product of nuclear reactors and nuclear explosions (Bentley et al. 1986; Phillips 2000). The use of  $^{36}\text{Cl}$  as a tracer of source in subduction zones is surprisingly limited. A  $^{36}\text{Cl}/\text{Cl}$  and  $^{129}\text{I}/\text{I}$  study of volcanic arc thermal springs and a non-thermal mineral spring in the fore-arc of the Cascade Range show that halogens discharged through these springs are primarily derived from magmatic sources, rather than underlying sedimentary units (Hurwitz et al. 2005). Br/Cl and I/Cl ratios and  $^{36}\text{Cl}$  and  $^{129}\text{I}$  data are consistent with halogens fluxed from the subducting slab (Hurwitz et al. 2005).

## 8.8 Summary

Our knowledge of the behavior of halogens in subduction zones has greatly increased in the last couple of decades. Chlorine stable isotopes and cosmogenic halogen isotopes ( $^{36}\text{Cl}$  and  $^{129}\text{I}$ ) have been employed to successfully trace fluid sources from subduction inputs to arc outputs. Serpentinites have been identified as major halogen sources, particularly for Cl ( $\sim 2000 \mu\text{g}/\text{g}$ ) and I (up to  $45 \mu\text{g}/\text{g}$ ), to sub-arc depths in subduction zones. High halogen concentrations in melt inclusions are strong evidence for the subduction of surficial reservoirs. Recent work on halogen concentrations in BABB and OIB also supports the survival of halogens into the upper mantle.

Despite these advances, halogen loss through the fore-arc and through hydrothermal systems is poorly constrained, leading to potentially large uncertainties in mass balance calculations. Our knowledge of the Cl cycle is the best understood, likely followed by F. Bromine and I arc outputs are poorly constrained with a few measurements from volcanic gas emissions and limited published data from melt inclusions. The extent to which these elements are lost to subduction-zone fluids and melts, and how they are fractionated from one another during subduction are areas of active research. The addition of halogens to aqueous slab fluids and the resultant effects on phase equilibria, as a function of the subduction geothermal gradient, may have profound implications for elemental transport within subduction zones.

**Acknowledgements** The authors thank M. Kendrick for discussions and providing a draft of Fig. 8.1, and R. Esposito for discussions on melt inclusions. The authors gratefully acknowledge thorough and helpful reviews by S. Straub, N. Metrich, and H. Marschall. We also thank D.E. Harlov and L. Aranovich for editorial handling, comments, and patience. This work was supported by the Deep Carbon Observatory and U.S. National Science Foundation grant EAR-1347987 to CEM.

## References

- Aiuppa A, Federico C, Franco A, Giudice G, Gurrieri S, Inguaggiato S, Liuzzo M, McGonigle AJS, Valenza M (2005) Emission of bromine and iodine from Mount Etna volcano. *Geochem Geophys Geosyst* 6:Q08008. <https://doi.org/08010.01029/02005GC000965>
- Aiuppa A, Baker DR, Webster JD (2009) Halogens in volcanic systems. *Chem Geol* 263:1–18
- Anderson G, Crear D (1993) *Thermodynamics in geochemistry*. Oxford University Press, New York, p 588
- Angiboust S, Agard P, Jolivet L, Beyssac O (2009) The Zermatt-Saas ophiolite: the largest (60-km wide) and deepest (c. 70–80 km) continuous slice of oceanic lithosphere detached from a subduction zone? *Terra Nova* 21:171–180
- Angiboust S, Langdon R, Agard P, Waters D, Chopin C (2012) Eclogitization of the Monviso ophiolite (W. Alps) and implications on subduction dynamics. *J Metamorph Geol* 30:37–61
- Anselmi B, Mellini M, Viti C (2000) Chlorine in the Elba, Monti Livornesi and Murlo serpentines: evidence for sea-water interaction. *Eur J Mineral* 12(1):137–146
- Aranovich LY, Newton RC (1996) H<sub>2</sub>O activity in concentrated solutions at high pressures and temperatures measured by the brucite-periclase equilibrium. *Contrib Mineral Petrol* 125:200–212
- Aranovich LY, Newton RC (1997) H<sub>2</sub>O activity in concentrated KCl and solutions at high temperatures and pressures measured by the brucite-periclase equilibrium. *Contrib Mineral Petrol* 127:261–271
- Aranovich LY, Newton RC (1999) Experimental determination of CO<sub>2</sub>-H<sub>2</sub>O activity-composition relations at 600–1000 C and 6–14 kbar by reversed decarbonation and dehydration reactions. *Am Mineral* 84(9):1319–1332
- Aranovich LY, Zakirov IV, Sretenskaya NG, Gerya TV (2010) Ternary system H<sub>2</sub>O-CO<sub>2</sub>-NaCl at high T-P parameters: an empirical mixing model. *Geochem Int* 48:446–455
- Aranovich LY, Newton RC, Manning CE (2013) Brine-assisted anatexis: experimental melting in the system haplogranite-H<sub>2</sub>O-NaCl-KCl at deep-crustal conditions. *Earth Planet Sci Lett* 374:111–120
- Arcuri T, Brimhall G (2003) The chloride source for atacamite mineralization at the Radomiro Tomic porphyry copper deposit, northern Chile. *Econ Geol* 98:1667–1681
- Aston FW (1920) The mass-spectra of chemical elements Part 2. *Philos Mag* 40:628–634
- Auer S, Bindeman I, Wallace P, Ponomareva V, Portnyagin M (2009) The origin of hydrous, high- $\delta^{18}\text{O}$  voluminous volcanism: diverse oxygen isotope values and high magmatic water contents within the volcanic record of Klyuchevskoy volcano, Kamchatka, Russia. *Contrib Mineral Petrol* 157:209–230
- Balcone-Boissard H, Villemant B, Boudon G (2010) Behavior of halogens during the degassing of felsic magmas. *Geochem Geophys Geosyst* 11:9
- Barnes JD, Cisneros M (2012) Mineralogical control on the chlorine isotope composition of altered oceanic crust. *Chem Geol* 326–327:51–60
- Barnes JD, Sharp ZD (2006) A chlorine isotope study of DSDP/ODP serpentinized ultramafic rocks: insights into the serpentinization process. *Chem Geol* 228:246–265
- Barnes JD, Straub SM (2010) Chlorine stable isotope variations in Izu Bonin tephra: implications for serpentinite subduction. *Chem Geol* 272:62–74

- Barnes JD, Selverstone J, Sharp ZD (2006) Chlorine chemistry of serpentinites from Elba, Italy, as an indicator of fluid source and subsequent tectonic history. *Geochem Geophys Geosyst* 7: Q08015. <https://doi.org/08010.01029/02006GC001296>
- Barnes JD, Sharp ZD, Fischer TP (2008) Chlorine isotope variations across the Izu-Bonin-Mariana arc. *Geology* 36:883–886
- Barnes JD, Paulick H, Sharp ZD, Bach W, Beaudoin G (2009a) Stable isotope ( $^{18}\text{O}$ , D,  $^{37}\text{Cl}$ ) evidence for multiple fluid histories in mid-Atlantic abyssal peridotites (ODP Leg 209). *Lithos* 110:83–94
- Barnes JD, Sharp ZD, Fischer TP, Hilton DR, Carr MJ (2009b) Chlorine isotope variations along the Central American volcanic front and back arc. *Geochem Geophys Geosyst* 10:Q11S17. <https://doi.org/10.1029/2009GC002587>
- Behn MD, Kelemen PB, Hirth G, Hacker BR, Massonne HJ (2011) Diapirs as the source of the sediment signature in arc lavas. *Nat Geosci* 4:641–646
- Benjamin ER, Plank T, Wade JA, Kelley KA, Hauri EH, Alvarado GE (2007) High water contents in basaltic magmas from Irazu Volcano, Costa Rica. *J Volcanol Geotherm Res* 168:68–92
- Bentley HW, Phillips FM, Davis SN (1986)  $^{36}\text{Cl}$  in the terrestrial environment. In: Fritz P, Fontes J-C (eds) *Handbook of environmental geochemistry*, vol 2b. Elsevier Science, New York, pp 422–475
- Bernini D, Wiedenbeck M, Dolejš D, Keppler H (2013) Partitioning of halogens between mantle minerals and aqueous fluids: implications for the fluid flow regime in subduction zones. *Contrib Miner Petrol* 165:117–128
- Beyer C, Klemme S, Wiedenbeck M, Stracke A, Vollmer C (2012) Fluorine in nominally fluorine-free mantle minerals: experimental partitioning of F between olivine, orthopyroxene and silicate melts with implications for magmatic processes. *Earth Planet Sci Lett* 337:1–9
- Bézos A, Escrig S, Langmuir CH, Michael PJ, Asimow PD (2009) Origins of chemical diversity of back-arc basin basalts: a segment-scale study of the Eastern Lau Spreading Center. *J Geophys Res* 114:B06212. <https://doi.org/06210.01029/02008JB005924>
- Bobrowski N, Hönninger G, Galle B, Platt U (2003) Detection of bromine monoxide in a volcanic plume. *Nature* 423:273–276
- Bonifacie M, Jendrzewski N, Agrinier P, Coleman M, Pineau F, Javoy M (2007a) Pyrohydrolysis-IRMS determination of silicate chlorine stable isotope compositions. Application to oceanic crust and meteorite samples. *Chem Geol* 242:187–201
- Bonifacie M, Monnin C, Jendrzewski N, Agrinier P, Javoy M (2007b) Chlorine stable isotopic composition of basement fluids of the eastern flank of the Juan de Fuca Ridge (ODP Leg 168). *Earth Planet Sci Lett* 260:10–22
- Bonifacie M, Busigny V, Mével C, Philippot P, Agrinier P, Jendrzewski N, Scambelluri M, Javoy M (2008a) Chlorine isotopic composition in seafloor serpentinites and high-pressure metaperidotites. Insights into oceanic serpentinization and subduction processes. *Geochim Cosmochim Acta* 72:126–139
- Bonifacie M, Jendrzewski N, Agrinier P, Humler E, Coleman M, Javoy M (2008b) The chlorine isotope composition of the Earth's mantle. *Science* 319:1518–1520
- Boschi C, Bonatti E, Ligi M, Brunelli D, Dallai L, D'Orazio M, Früh-Green G, Tonarini S, Barnes JD, Bedini R (2013) A 10 Ma year old window into deep hydrothermal circulation at the Vema Fracture Zone (11°N, MAR). *Lithos* 178:3–23
- Bostock MG, Hyndman RD, Rondenay S, Peacock SM (2002) An inverted continental Moho and serpentinization of the forearc mantle. *Nature* 417:536–538
- Bucher K, Fazis Y, Capitani CD, Grapes R (2005) Blueschists, eclogites, and decompression assemblages of the Zermatt-Saas ophiolite: high-pressure metamorphism of subducted Tethys lithosphere. *Am Mineral* 90:821–835
- Bucholz CE, Gaetani GA, Behn MD, Shimizu N (2013) Post-entrapment modification of volatiles and oxygen fugacity in olivine-hosted melt inclusions. *Earth Planet Sci Lett* 374:145–155
- Bureau H, Keppler H, Métrich N (2000) Volcanic degassing of bromine and iodine: experimental fluid/melt partitioning data and applications to stratospheric chemistry. *Earth Planet Sci Lett* 183:51–60

- Burgess R, Layzelle E, Turner G, Harris JW (2002) Constraints on the age and halogen composition of mantle fluids in Siberian coated diamonds. *Earth Planet Sci Lett* 197:193–203
- Cannaò E, Agostini S, Scambelluri M, Tonarini S, Godard M (2015) B, Sr and Pb isotope geochemistry of high-pressure Alpine metaperidotites monitors fluid-mediated element recycling during serpentinite dehydration in subduction mélange (Cima di Gagnone, Swiss Central Alps). *Geochim Cosmochim Acta* 163:80–100
- Cannat M, Karson JA, Miller DJ, et al (1995) Proc. ODP, Init. Repts. In, vol 153. Ocean Drilling Program, College Station, TX, p 798
- Cervantes P, Wallace PJ (2003) Role of H<sub>2</sub>O in subduction-zone magmatism: new insights from melt inclusions in high-Mg basalts from central Mexico. *Geology* 31:235–238
- Chiaradia M, Barnes JD, Cadet-Voisin S (2014) Chlorine isotope variations across the Quaternary volcanic arc of Ecuador. *Earth Planet Sci Lett* 396:22–33
- Clift P, Vannucchi P (2004) Controls on tectonic accretion versus erosion in subduction zones: implications for the origin and recycling of the continental crust. *Rev Geophys* 42:1
- Dalou C, Koga KT, Shimizu N, Boulon J, Devidal JL (2012) Experimental determination of F and Cl partitioning between lherzolite and basaltic melt. *Contrib Mineral Petrol* 163:591–609
- Davies JH, Stevenson DJ (1992) Physical model for the source region of subduction zone volatiles. *J Geophys Res* 97:2037–2070
- Debret B, Nicollet C, Andreani M, Schwartz S, Godard M (2013) Three steps of serpentinisation in an eclogitized oceanic serpentinization front (Lanzo Massif—Western Alps). *J Metamorph Geol* 31:165–186
- Debret B, Koga KT, Nicollet C, Andreani M, Schwartz S (2014) F, Cl and S input via serpentinite in subduction zones: implications for the nature of the fluid released at depth. *Terra Nova* 26:96–101
- Debret B, Koga KT, Cattani F, Nicollet C, Van den Bleeken G, Schwartz S (2016) Volatile (Li, B, F and Cl) mobility during amphibole breakdown in subduction zones. *Lithos* 244:165–181
- Deruelle B, Dreibus G, Jambon A (1992) Iodine abundances in oceanic basalts: implications for Earth dynamics. *Earth Planet Sci Lett* 108:217–227
- Deschamps F, Godard M, Guillot S, Hattori K (2013) Geochemistry of subduction zone serpentinites: a review. *Lithos* 178:96–127
- Eastoe CJ, Peryt T (1999) Stable chlorine isotope evidence for non-marine chloride in Badenian evaporites, Carpathian mountain region. *Terra Nova* 11(2/3):118–123
- Eastoe CJ, Long A, Knauth LP (1999) Stable chlorine isotopes in the Palo Duro Basin, Texas: evidence for preservation of Permian evaporite brines. *Geochim Cosmochim Acta* 63(9): 1375–1382
- Eastoe CJ, Peryt TM, Petrychenko OY, Geisler-Cussey D (2007) Stable chlorine isotopes of Phanerozoic evaporites. *Appl Geochem* 22:575–588
- Eggenkamp HGM, Kreulen R, Koster van Groos AF (1995) Chloride stable isotope fractionation in evaporites. *Geochim Cosmochim Acta* 59(24):5169–5175
- Eiler JM, Carr MJ, Reagan M, Stolper E (2005) Oxygen isotope constraints on the sources of Central American arc lavas. *Geochem Geophys Geosyst* 6:Q07007. <https://doi.org/10.1029/2004GC000804>
- Espósito R, Hunter J, Schiffbauer JD, Shimizu N, Bodnar RJ (2014) An assessment of the reliability of melt inclusions as recorders of the pre-eruptive volatile content of magmas. *Am Mineral* 99:976–998
- Evans BW, Trommsdorff V (1978) Petrogenesis of garnet lherzolite, Cima di Gagnone, Lepontine Alps. *Earth Planet Sci Lett* 40:333–348
- Evans BW, Trommsdorff V (1983) Fluorine hydroxyl titanian clinohumite in Alpine recrystallized garnet peridotite: compositional controls and petrologic significance. *Am J Sci* 283:355–369
- Fabbrizio A, Stalder R, Hametner K, Günther D, Marquardt K (2013) Experimental partitioning of halogens and other trace elements between olivine, pyroxenes, amphibole and aqueous fluid at 2 GPa and 900–1,300 °C. *Contrib Mineral Petrol* 166:639–653
- Fabryka-Martin J, Bentley J, Elmore D, Airey PL (1985) Natural iodine-129 as an environmental tracer. *Geochim Cosmochim Acta* 49:337–347

- Fehn U (2012) Tracing crustal fluids: applications of natural  $^{129}\text{I}$  and  $^{36}\text{Cl}$ . *Ann Rev Earth Planet Sci* 40:45–67
- Fehn U, Snyder GT (2003) Origin of iodine and  $^{129}\text{I}$  in volcanic and geothermal fluids from the North Island of New Zealand: implications for Subduction Zone Processes. *Spec Publ Soc Econ Geol* 10:159–170
- Fehn U, Snyder GT, Varekamp JC (2002) Detection of recycled marine sediment components in crater lake fluids using  $^{129}\text{I}$ . *J Volcanol Geotherm Res* 115:451–460
- Fehn U, Lu Z, Tomaru H (2006)  $^{129}\text{I}/\text{I}$  ratios and halogen concentrations in pore water of Hydrate Ridge and their relevance for the origin of gas hydrates: a progress report. In: Trehu AM, Bohrmann G, Torres ME, Colwell FS (eds) *Proceedings of the ocean drilling program, Scientific results, vol 204*, pp 1–25
- Fehn U, Snyder GT, Muramatsu Y (2007) Iodine as a tracer of organic material:  $^{129}\text{I}$  results from gas hydrate systems and fore arc fluids. *J Geochem Explor* 95:66–80
- Fischer TP (2008) Fluxes of volatiles ( $\text{H}_2\text{O}$ ,  $\text{CO}_2$ ,  $\text{N}_2$ ,  $\text{Cl}$ ,  $\text{F}$ ) from arc volcanoes. *Geochem J* 42:21–38
- Fischer TP, Hilton DR, Zimmer MM, Shaw AM, Sharp ZD, Walker JA (2002) Subduction and recycling of nitrogen along the Central American margin. *Science* 297:1154–1157
- Gaetani GA, O’Leary JA, Shimizu N, Bucholz CE, Newville M (2012) Rapid reequilibration of  $\text{H}_2\text{O}$  and oxygen fugacity in olivine-hosted melt inclusions. *Geology* 40:915–918
- Gao S, Luo TC, Zhang BR, Zhang HF, Han YW, Zhao ZD, Hu YK (1998) Chemical composition of the continental crust as revealed by studies in East China. *Geochim Cosmochim Acta* 62:1959–1975
- Gerya TV, Yuen DA (2003) Rayleigh-Taylor instabilities from hydration and melting propel ‘cold plumes’ at subduction zones. *Earth Planet Sci Lett* 212:47–62
- Gillis KM (1996) Rare element constraints on the origin of amphibole in gabbroic rocks from Site 894, Hess Deep. In: Mevel C, Gillis KM, Allan JF, Meyer PS (eds) *Proceedings of the ocean drilling program, Scientific results, vol 147. Ocean Drilling Program*, pp 59–75
- Gillis KM, Meyer PS (2001) Metasomatism of oceanic gabbros by late stage melts and hydrothermal fluids: evidence from rare earth element composition of amphiboles. *Geochem Geophys Geosyst* 2:2000GC000087
- Godon A, Jendrzewski N, Castrec-Rouelle M, Dia A, Pineau F, Boulègue J, Javoy M (2004) Origin and evolution of fluids from mud volcanoes in the Barbados accretionary complex. *Geochim Cosmochim Acta* 68(9):2153–2165
- Hacker BR (2008)  $\text{H}_2\text{O}$  subduction beyond arcs. *Geochem Geophys Geosyst* 9:Q03001. <https://doi.org/03010.01029/02007GC001707>
- Halbach H, Chatterjee ND (1982) An empirical Redlich-Kwong-type equation of state for water to 1000 °C and 200 kbar. *Contrib Mineral Petrol* 79:337–345
- Harvey J, Garrido CJ, Savov I, Agostini S, Padrón-Navarta JA, Marchesi C, Sánchez-Vizcaíno VL, Gómez-Pugnaire MT (2014)  $^{11}\text{B}$ -rich fluids in subduction zones: the role of antigorite dehydration in subducting slabs and boron isotope heterogeneity in the mantle. *Chem Geol* 376:20–30
- Heinrich W (2007) Fluid immiscibility in metamorphic rocks. *Rev Mineral Geochem* 65:389–430
- Hermann J, Müntener O, Scambelluri M (2000) The importance of serpentinite mylonites for subduction and exhumation of oceanic crust. *Tectonophysics* 327:225–238
- Hoernle K, Abt DL, Fischer KM, Nichols H, Hauff F, Abers GA, van den Bogaard P, Heydolph K, Alvarado G, Protti M, Strauch W (2008) Arc-parallel flow in the mantle wedge beneath Costa Rica and Nicaragua. *Nature* 451:1094–1097
- Hofmann AW (2003) Sampling mantle heterogeneity through oceanic basalts: isotopes and trace elements. In: Carlson RL (ed) *The core and mantle: treatise on geochemistry, vol 2*. Elsevier Ltd., Oxford, pp 61–101
- Holloway JR (1977) *Fugacity and activity of molecular species in supercritical fluids, vol 10*. Springer, New York

- Hurwitz S, Mariner RH, Fehn U, Snyder GT (2005) Systematics of halogen elements and their radioisotopes in thermal springs of the Cascade Range, Central Oregon, Western USA. *Earth Planet Sci Lett* 235:700–714
- Hyndman RD, Peacock SM (2003) Serpentinization of the forearc mantle. *Earth Planet Sci Lett* 212:417–432
- Ishizuka H (1989) Mineral paragenesis of altered basalts from Hole 504B, ODP Leg 111. In: Becker K, Sakai H, et al (eds) *Proceedings of the ocean drilling program, Scientific results, vol. Ocean Drilling Program*, pp 61–76
- Ito E, Harris DM, Anderson AT Jr (1983) Alteration of oceanic crust and geologic recycling of chlorine and water. *Geochim Cosmochim Acta* 47:1613–1624
- Jambon A, Déruelle B, Dreibus G, Pineau F (1995) Chlorine and bromine abundance in MORB: the contrasting behaviour of the Mid-Atlantic Ridge and East Pacific Rise and implications for chlorine geodynamic cycle. *Chem Geol* 126:101–117
- Jarrard RD (2003) Subduction fluxes of water, carbon dioxide, chlorine, and potassium. *Geochem Geophys Geosyst* 4(5):8905. <https://doi.org/8910.1029/2002GC000392>
- John T, Layne GD, Haase KM, Barnes JD (2010) Chlorine isotope evidence for crustal recycling into the Earth's mantle. *Earth Planet Sci Lett* 298:175–182
- John T, Scambelluri M, Frische M, Barnes JD, Bach W (2011) Dehydration of subducting serpentinite: implications for halogen mobility in subduction zones and the deep halogen cycle. *Earth Planet Sci Lett* 308(1):65–76. <https://doi.org/10.1016/j.epsl.2011.1005.1038>
- Johnson ER, Wallace PJ, Granados HD, Manea VC, Kent AJ, Bindeman IN, Donegan CS (2009) Subduction-related volatile recycling and magma generation beneath Central Mexico: insights from melt inclusions, oxygen isotopes and geodynamic models. *J Petrol* 50:1729–1764
- Kastner M, Elderfield H, Martin JB (1991) Fluids in convergent margins: what do we know about their composition, origin, role in diagenesis and importance for oceanic chemical fluxes? *Philos Trans R Soc Lond* 335:243–259
- Kaufmann R, Long A, Bentley H, Davis S (1984) Natural chlorine isotope variations. *Nature* 309:338–340
- van Keken PE, Hacker BR, Syracuse EM, Abers GA (2011) Subduction factory: 4. Depth-dependent flux of H<sub>2</sub>O from subducting slabs worldwide. *J Geophys Res* 116: B01401. <https://doi.org/01410.01029/02010JB007922>
- Kelemen PB, Manning CE (2015) Reevaluating carbon fluxes in subduction zones, what goes down, mostly comes up. *Proc Natl Acad Sci*. <https://doi.org/10.1073/pnas.1507889112>
- Kendrick MA, Scambelluri M, Honda M, Phillips D (2011) High abundances of noble gas and chlorine delivered to the mantle by serpentinite subduction. *Nat Geosci* 4(11):807–812
- Kendrick MA, Kamenetsky VS, Phillips D, Honda M (2012a) Halogen systematics (Cl, Br, I) in mid-ocean ridge basalts: a Macquarie Island case study. *Geochim Cosmochim Acta* 81:82–93
- Kendrick MA, Woodhead JD, Kamenetsky VS (2012b) Tracking halogens through the subduction cycle. *Geology* 40:1075–1078
- Kendrick MA, Honda M, Pettke T, Scambelluri M, Phillips D, Giuliani A (2013) Subduction zone fluxes of halogens and noble gases in seafloor and forearc serpentinites. *Earth Planet Sci Lett* 365:86–96
- Kendrick MA, Arculus RJ, Danyushevsky LV, Kamenetsky VS, Woodhead JD, Honda M (2014a) Subduction-related halogens (Cl, Br and I) and H<sub>2</sub>O in magmatic glasses from Southwest Pacific Backarc Basins. *Earth Planet Sci Lett* 400:165–176
- Kendrick MA, Jackson MG, Kent AJ, Hauri EH, Wallace PJ, Woodhead J (2014b) Contrasting behaviours of CO<sub>2</sub>, S, H<sub>2</sub>O and halogens (F, Cl, Br, and I) in enriched-mantle melts from Pitcairn and Society seamounts. *Chem Geol* 370:69–81
- Kent AJR, Peate DW, Newman S, Stolper EM, Pearce JA (2002) Chlorine in submarine glasses from the Lau Basin: seawater contamination and constraints on the composition of slab-derived fluids. *Earth Planet Sci Lett* 202:361–377
- Keppler H (1996) Constraints from partitioning experiments on the composition of subduction-zone fluids. *Nature* 380:237–240
- Keppler H (2017) Fluids and trace element transport in subduction zones. *Am Mineral* 102:5–20
- Kerrick D, Jacobs G (1981) A modified Redlich-Kwong equation for H<sub>2</sub>O, CO<sub>2</sub>, and H<sub>2</sub>O-CO<sub>2</sub> mixtures at elevated pressures and temperatures. *Am J Sci* 281(6):735–767
- Kerrick DM (2002) Serpentine seduction. *Science* 298:1344–1345

- Klemme S, Stalder R (2018) Halogens in the Earth's mantle: what we know and what we don't. In: Harlov DE, Aranovich L (eds) The role of halogens in terrestrial and extraterrestrial geochemical processes: surface, crust, and mantle. Springer, Berlin, pp 847–869
- Kodolányi J, Pettke T (2011) Loss of trace elements from serpentinites during fluid-assisted transformation of chrysotile to antigorite—an example from Guatemala. *Chem Geol* 284:351–362
- Kodolányi J, Pettke T, Spandler C, Kamber BS, Gméling K (2012) Geochemistry of ocean floor and fore-arc serpentinites: constraints on the ultramafic input to subduction zones. *J Petrol* 53:235–270
- Kutterolf S, Hansteen TH, Appel K, Freundt A, Krüger K, Perez W, Wehrmann H (2013) Combined bromine and chlorine release from large explosive volcanic eruptions: a threat to stratospheric ozone? *Geology* 41:707–710
- Lafay R, Deschamps F, Schwartz S, Guillot S, Godard M, Debret B, Nicollet C (2013) High-pressure serpentinites, a trap-and-release system controlled by metamorphic conditions: example from the Piedmont zone of the western Alps. *Chem Geol* 343:38–54
- Lagabrielle Y, Cannat M (1990) Alpine Jurassic ophiolites resemble the modern central Atlantic basement. *Geology* 18(4):319–322
- Lassiter JC, Hauri EH, Nikogosian IK, Barszczus HG (2002) Chlorine-potassium variations in melt inclusions from Raivavae and Rapa, Austral Islands: constraints on chlorine recycling in the mantle and evidence for brine-induced melting of oceanic crust. *Earth Planet Sci Lett* 202:525–540
- Laverne C, Vanko DA, Tartarotti P, Alt JC (1995) Chemistry and geothermometry of secondary minerals from the deep sheeted dike complex, Hole 504B. In: Erzinger J, Becker K, Dick HJB, Stokking LB (eds) Proceedings of the ocean drilling program, Scientific results, vol 137/140. Ocean Drilling Program, pp 167–189
- Layne GD, Kent AJR, Bach W (2009)  $\delta^{37}\text{Cl}$  systematics of a backarc spreading system: the Lau Basin. *Geology* 37:427–430
- Li XP, Rahn M, Bucher K (2004) Serpentinites of the Zermatt-Saas ophiolite complex and their texture evolution. *J Metamorph Geol* 22:159–177
- Li Y-H (1982) A brief discussion on the mean oceanic residence time of elements. *Geochim Cosmochim Acta* 46:2671–2675
- Li Y-H, Schoemaker JE (2003) Chemical composition and mineralogy of marine. *Treatise Geochem* 7:1–35
- Liebscher A (2010) Aqueous fluids at elevated pressure and temperature. *Geofluids* 10:3–19
- Lopez Sánchez-Vizcaino VL, Trommsdorff V, Gómez-Pugnaire MT, Garrido CJ, Müntener O, Connolly JAD (2005) Petrology of titanian clinohumite and olivine at the high-pressure breakdown of antigorite serpentinite to chlorite harzburgite (Almirez Massif, S. Spain). *Contrib Mineral Petrol* 149:627–646
- Luth R (2014) Volatiles in Earth's Mantle. In: Holland HD, Turekian KK (eds) *Treatise on Geochemistry*, vol 3, 2nd edn. Elsevier, Oxford, pp 355–379
- Manning CE (2004) The chemistry of subduction-zone fluids. *Earth Planet Sci Lett* 223:1–16
- Manning CE (2013) Thermodynamic modeling of fluid-rock interaction at conditions of the earth's middle crust to upper mantle. *Rev Mineral Geochem* 76:135–164
- Manning CE, Aranovich LY (2014) Brines at high pressure and temperature: thermodynamic, petrologic and geochemical effects. *Precambr Res* 253:6–16
- Manning CE, Shock EL, Sverjensky DA (2013) The chemistry of carbon in aqueous fluids at crustal and upper-mantle conditions: experimental and theoretical constraints. *Rev Mineral Geochem* 75:109–148
- Mantegazzi D, Sanchez-Valle C, Driesner T (2013) Thermodynamic properties of aqueous solutions to 1073 K and 4.5 GPa, and implications for dehydration reactions in subducting slabs. *Geochim Cosmochim Acta* 121:263–290
- Marschall HR, Schumacher JC (2012) Arc magmas sourced from mélange diapirs in subduction zones. *Nat Geosci* 5:862–867

- Marschall HR, Altherr R, Gmélíng K, Kasztovszky ZS (2009) Lithium, boron and chlorine as tracers for metasomatism in high-pressure metamorphic rocks: a case study from Syros (Greece). *Mineral Petrol* 95:291–302
- Martin JB, Gieskes JM, Torres M, Kastner M (1993) Bromine and iodine in Peru margin sediments and: implications for fluid origins. *Geochim Cosmochim Acta* 57:4377–4389
- Métrich N, Deloué E (2014) Water content,  $\delta D$  and  $\delta^{11}B$  tracking in the Vanuatu arc magmas (Aoba Island): insights from olivine-hosted melt inclusions. *Lithos* 206:400–408
- Mével C (2003) Serpentinization of abyssal peridotites at mid-ocean ridges. *C R Geosci* 335:825–852
- Michael PJ, Cornell WC (1998) Influence of spreading rate and magma supply on crystallization and assimilation beneath mid-ocean ridges: evidence from chlorine and major element chemistry of mid-ocean ridge basalts. *J Geophys Res* 103(B8):18325–18356
- Michael PJ, Schilling J-G (1989) Chlorine in mid-ocean ridge magmas: evidence for assimilation of seawater-influenced components. *Geochim Cosmochim Acta* 53:3131–3143
- Morrison J (1991) Compositional constraints on the incorporation of Cl into amphiboles. *Am Mineral* 76:1920–1930
- Mottl MJ, Wheat CG, Fryer P, Gharib J, Martin JB (2004) Chemistry of springs across the Mariana forearc shows progressive devolatilization of the subducting plate. *Geochim Cosmochim Acta* 68:4915–4933
- Munoz JL (1984) F-OH and Cl-OH exchange in micas with applications to hydrothermal ore deposits. In: Bailey SW (ed) *Reviews in mineralogy: micas*, vol 13. Mineralogical Society of America, Washington, D.C., p 584
- Muramatsu Y, Ohmomo Y (1986) Iodine-129 and iodine-127 in environmental samples collected from Tokaimura/Ibaraki, Japan. *Sci Total Environ* 48:33–43
- Muramatsu Y, Wedepohl KH (1998) The distribution of iodine in the earth's crust. *Chem Geol* 147:201–216
- Muramatsu Y, Fehn U, Yoshida S (2001) Recycling of iodine in fore-arc areas: evidence from the iodine brines in Chiba, Japan. *Earth Planet Sci Lett* 192:583–593
- Muramatsu Y, Doi T, Tomaru H, Fehn U, Takeuchi R, Matsumoto R (2007) Halogen concentrations in pore waters and sediments of the Nankai Trough, Japan: implications for the origin of gas hydrates. *Appl Geochem* 22:534–556
- Nehlig P (1993) Interactions between magma chambers and hydrothermal systems: oceanic and ophiolitic constraints. *J Geophys Res Solid Earth* 98(B11):19621–19633
- Oelkers EH, Helgeson HC (1993) Multiple ion association in supercritical aqueous solutions of single electrolytes. *Science* 261:888–891
- Padrón-Navarta JA, Tommasi A, Garrido CJ, Lopez Sanchez-Vizcaino V, Gómez-Pugnaire MT, Jabaloy A, Vauchez A (2010) Fluid transfer into the wedge controlled by high-pressure hydrofracturing in the cold top-slab mantle. *Earth Planet Sci Lett* 297:271–286
- Patino LC, Carr MJ, Feigenson MD (2000) Local and regional variations in Central American arc lavas controlled by variations in subducted sediment input. *Contrib Mineral Petrol* 138:265–283
- Pelletier L, Müntener O (2006) High-pressure metamorphism of the Lanzo peridotite and its oceanic cover, and some consequences for the Sesia-Lanzo zone (northwestern Italian Alps). *Lithos* 90:111–130
- Pertsev AN, Aranovich LY, Prokofiev VY, Bortnikov NS, Cipriani A, Simakin SS, Borisovskiy SE (2015) Signatures of residual melts, magmatic and seawater-derived fluids in oceanic lower-crust gabbro from the vema lithospheric section, central Atlantic. *J Petrol* 56:1069–1088
- Philippot P, Selverstone J (1991) Trace-element-rich brines in eclogitic veins: implications for fluid composition and transport during subduction. *Contrib Mineral Petrol* 106:417–430
- Philippot P, Agrinier P, Scambelluri M (1998) Chlorine cycling during subduction of altered oceanic crust. *Earth Planet Sci Lett* 161(1–4):33–44
- Phillips FM (2000) Chlorine-36. In: Cook PG, Herczeg AL (eds) *Environmental tracers in subsurface hydrology*. Kluwer Academic Publishing, Boston, pp 299–348

- Pieri D (2015) Satellite and aircraft-based techniques to measure volcanic emissions and hazards. In: Schmidt A, Fristad K, Elkins-Tanton L (eds) *Volcanism and global environmental change*. Cambridge University Press, Cambridge, pp 133–146
- Platt U, Bobrowski N (2015) Quantification of volcanic reactive halogen emissions. In: Schmidt A, Fristad K, Elkins-Tanton L (eds) *Volcanism and global environmental change*. Cambridge University Press, Cambridge, pp 111–132
- Portnyagin M, Hoernle K, Plechov P, Mironov N, Khubunaya S (2007) Constraints on mantle melting and composition and nature of slab components in volcanic arcs from volatiles (H<sub>2</sub>O, S, Cl, F) and trace elements in melt inclusions from the Kamchatka Arc. *Earth Planet Sci Lett* 255:53–69
- Portnyagin M, Almeev R, Matveev S, Holtz F (2008) Experimental evidence for rapid water exchange between melt inclusions in olivine and host magma. *Earth Planet Sci Lett* 272:541–552
- Pyle DM, Mather TA (2009) Halogens in igneous processes and their fluxes to the atmosphere and oceans from volcanic activity: a review. *Chem Geol* 263:110–121
- Ranero CR, Morgan JP, McIntosh K, Reichert C (2003) Bending-related faulting and mantle serpentinization at the Middle America trench. *Nature* 425:367–373
- Ransom B, Spivack AJ, Kastner M (1995) Stable Cl isotopes in subduction-zone pore waters: implications for fluid-rock reactions and the cycling of chlorine. *Geology* 23(8):715–718
- Rebay G, Spalla MI, Zanon D (2012) Interaction of deformation and metamorphism during subduction and exhumation of hydrated oceanic mantle: insights from the Western Alps. *J Metamorph Geol* 30:687–702
- Roggensack K, Hervig RL, McKnight SB, Williams SN (1997) Explosive basaltic volcanism from Cerro Negro volcano: influence of volatiles on eruptive style. *Science* 277:1639–1642
- Rüpke LH, Morgan JP, Hort M, Connolly JAD (2004) Serpentine and the subduction zone water cycle. *Earth Planet Sci Lett* 223:17–24
- Ruscitto DM, Wallace PJ, Johnson ER, Kent AJR, Bindeman IN (2010) Volatile contents of mafic magmas from cinder cones in the Central Oregon High Cascades: implications for magma formation and mantle conditions in a hot arc. *Earth Planet Sci Lett* 298:153–161
- Ruscitto DM, Wallace PJ, Cooper LB, Plank T (2012) Global variations in H<sub>2</sub>O/Ce: 2. Relationships to arc magma geochemistry and volatile fluxes. *Geochem Geophys Geosyst* 13: Q03025
- Ryan JG, Chauvel C (2014) The subduction-zone filter and the impact of recycled materials on the evolution of the mantle. In: Holland HD, Turekian KK (eds) *The mantle and core*. Treatise on geochemistry, vol 3. Elsevier, Oxford, pp 479–508
- Saal AE, Hauri EH, Langmuir CH, Perfit MR (2002) Vapour undersaturation in primitive mid-ocean-ridge basalt and the volatile content of the Earth's upper mantle. *Nature* 419:451–455
- Sadofsky SJ, Portnyagin M, Hoernle K, van den Bogaard P (2008) Subduction cycling of volatiles and trace elements through the Central American volcanic arc: evidence from melt inclusions. *Contrib Mineral Petrol* 155:433–456
- Sakuma H, Ichiki M (2015) Density and isothermal compressibility of supercritical H<sub>2</sub>O-NaCl fluid: molecular dynamics study from 673 to 2000 K, 0.2 to 2 GPa, and 0 to 22 wt% NaCl concentrations. *Geofluids* 16(2016):89–102
- Salters VJM, Stracke A (2004) Composition of the depleted mantle. *Geochem Geophys Geosyst* 5: Q05B07. <https://doi.org/10.1029/2003GC000597>
- Sano T, Miyoshi M, Ingle S, Banerjee NR, Ishimoto M, Fukuoka T (2008) Boron and chlorine contents of upper oceanic crust: basement samples from IODP Hole 1256D. *Geochem Geophys Geosyst* 9:Q12015. <https://doi.org/10.1029/2008GC002182>
- Savov IP, Ryan JG, D'Antonio M, Kelley K, Mattie P (2005) Geochemistry of serpentinized peridotites from the Mariana forearc Conical seamounts, ODP Leg 125: implications for the elemental recycling at subduction zones. *Geochem Geophys Geosyst* 6:4
- Saxena SK, Fei Y (1987) High pressure and high temperature fluid fugacities. *Geochim Cosmochim Acta* 51:783–791

- Scambelluri M, Philippot P (2001) Deep fluids in subduction zones. *Lithos* 55:213–227
- Scambelluri M, Tonarini S (2012) Boron isotope evidence for shallow fluid transfer across subduction zones by serpentinitized mantle. *Geology* 40:907–910
- Scambelluri M, Muntener O, Hermann J, Piccardo GB, Trommsdorff V (1995) Subduction of water into the mantle: history of an alpine peridotite. *Geology* 23(5):459–462
- Scambelluri M, Piccardo GB, Philippot P, Robbiano A, Negretti L (1997) High salinity fluid inclusions formed from recycled seawater in deeply subducted alpine serpentinite. *Earth Planet Sci Lett* 148(3–4):485–499
- Scambelluri M, Bottazzi P, Trommsdorff V, Vannucci R, Hermann J, Gomez-Pugnaire MT, Vizcaino VLS (2001) Incompatible element-rich fluids released by antigorite breakdown in deeply subducted mantle. *Earth Planet Sci Lett* 192(3):457–470
- Scambelluri M, Müntener O, Ottolini L, Pettker TT, Vannucci R (2004) The fate of B, Cl and Li in the subducted oceanic mantle and in the antigorite breakdown fluids. *Earth Planet Sci Lett* 222:217–234
- Scambelluri M, Pettker T, Rampone E, Godard M, Reusser E (2014) Petrology and trace element budgets of high-pressure peridotites indicate subduction dehydration of serpentinitized mantle (Cima di Gagnone, Central Alps, Switzerland). *J Petrol* 55:459–498
- Schauble EA, Rossman GR, Taylor HPJ (2003) Theoretical estimates of equilibrium chlorine-isotope fractionations. *Geochim Cosmochim Acta* 67(17):3267–3281
- Schilling J-G, Bergeron MB, Evans R (1980) Halogens in the mantle beneath the North Atlantic. *Phil Trans R Soc Lond A297*:147–178
- Schmidt MW, Poli S (1998) Experimentally based water budgets for dehydrating slabs and consequences for arc magma generation. *Earth Planet Sci Lett* 163:361–379
- Scholl DW, von Huene R (2007) Crustal recycling at modern subduction zones applied to the past — issues of growth and preservation of continental basement crust, mantle geochemistry, and supercontinent reconstruction. *Geol Soc Am Mem* 200:9–32
- Selverstone J, Sharp ZD (2011) Chlorine isotope evidence for multicomponent mantle metasomatism in the Ivrea Zone. *Earth Planet Sci Lett* 310:429–440
- Selverstone J, Sharp ZD (2013) Chlorine isotope constraints on fluid-rock interactions during subduction and exhumation of the Zermatt-Saas ophiolite. *Geochem Geophys Geosyst* 14: 4370–4391. <https://doi.org/10.1002/ggge.20269>
- Selverstone J, Sharp ZD (2015) Chlorine isotope behavior during prograde metamorphism of sedimentary rocks. *Earth Planet Sci Lett* 417:120–131
- Selverstone J, Franz G, Thomas S, Getty S (1992) Fluid variability in 2 GPa eclogites as an indicator of fluid behavior during subduction. *Contrib Mineral Petrol* 112:341–357
- Sharp ZD, Barnes JD (2004) Water soluble chlorides in massive seafloor serpentinites: a source of chloride in subduction zones. *Earth Planet Sci Lett* 226:243–254
- Sharp ZD, Barnes JD, Brearley AJ, Chaussidon M, Fischer TP, Kamenetsky VS (2007) Chlorine isotope homogeneity of the mantle, crust and carbonaceous chondrites. *Nature* 446:1062–1065
- Sharp ZD, Barnes JD, Fischer TP, Halick M (2010) A laboratory determination of chlorine isotope fractionation in acid systems and applications to volcanic fumaroles. *Geochim Cosmochim Acta* 74:264–273
- Sharp ZD, Mercer JA, Jones RH, Brearley AJ, Selverstone J, Bekker A, Stachel T (2013) The chlorine isotope composition of chondrites and earth. *Geochim Cosmochim Acta* 107:189–204
- Shaw AM, Hauri EH, Fischer TP, Hilton DR, Kelley KA (2008) Hydrogen isotopes in Mariana arc melt inclusions: implications for subduction dehydration and the deep-Earth water cycle. *Earth Planet Sci Lett* 275:138–145
- Shinohara H (2008) Excess degassing from volcanoes and its role on eruptive and intrusive activity. *Rev Geophys* 46:1–31
- Shinohara H (2013) Volatile flux from subduction zone volcanoes: insights from a detailed evaluation of the fluxes from volcanoes in Japan. *J Volcanol Geotherm Res* 268:46–63
- Shmulovich KI, Graham CM (1996) Melting of albite and dehydration of brucite in H<sub>2</sub>O-NaCl fluids to 9 kbars and 700–900 °C: implications for partial melting and water activities during high pressure metamorphism. *Contrib Mineral Petrol* 124(3–4):370–382

- Sisson TW, Bronto S (1998) Evidence for pressure-release melting beneath magmatic arcs from basalt at Galunggung, Indonesia. *Nature* 391:883–886
- Snyder GT, Fehn U (2002) Origin of iodine in volcanic fluids:  $^{129}\text{I}$  results from the Central American Volcanic Arc. *Geochim Cosmochim Acta* 66:3827–3838
- Snyder GT, Savov IP, Muramatsu Y (2005) Iodine and boron in Mariana serpentinite mud volcanoes (ODP Legs 125 and 195): Implications for forearc processes and subduction recycling. *Proceedings of the ocean drilling program, Scientific results 195*
- Spivack AJ, Kastner M, Ransom B (2002) Elemental and isotopic chloride geochemistry and fluid flow in the Nankai Trough. *Geophys Res Lett* 29(14):6-1–6-4
- Stolper EM, Newman S (1994) The role of water in the petrogenesis of Mariana trough magmas. *Earth Planet Sci Lett* 121:293–325
- Straub SM, Layne GD (2003) The systematics of chlorine, fluorine, and water in Izu arc front volcanic rocks: implications for volatile recycling in subduction zones. *Geochim Cosmochim Acta* 67(21):4179–4203
- Stronck NA, Haase KM (2004) Chlorine in oceanic intraplate basalts: constraints on mantle sources and recycling processes. *Geology* 32:945–948
- Stueber AM, Huang WH, Johns WD (1968) Chlorine and fluorine abundances in ultramafic rocks. *Geochim Cosmochim Acta* 32:353–358
- Sumino H, Burgess R, Mizukami T, Wallis SR, Holland G, Ballentine CJ (2010) Seawater-derived noble gases and halogens preserved in exhumed mantle wedge peridotite. *Earth Planet Sci Lett* 294:163–172
- Sun WD, Binns RA, Fan AC, Kamenetsky VS, Wysoczanski R, Wei GJ, Hu YH, Arculus RJ (2007) Chlorine in submarine volcanic glasses from the eastern Manus basin. *Geochim Cosmochim Acta* 71:1542–1552
- Sverjensky DA, Harrison B, Azzolini D (2014) Water in the deep Earth: the dielectric constant and the solubilities of quartz and corundum to 60 kb and 1200 °C. *Geochim Cosmochim Acta* 129:125–145
- Symonds RB, Rose WI, Reed MH (1988) Contribution of Cl- and F-bearing gases to the atmosphere by volcanoes. *Nature* 334:415–418
- Syracuse EM, van Keken PE, Abers GA (2010) The global range of subduction zone thermal models. *Phys Earth Planet Inter* 183(1–2):73–90
- Taran YA (2009) Geochemistry of volcanic and hydrothermal fluids and volatile budget of the Kamchatka-Kuril subduction zone. *Geochim Cosmochim Acta* 73:1067–1094
- Tatsumi Y (1986) Formation of the volcanic front in subduction zones. *Geophys Res Lett* 17:717–720
- Tatsumi Y (1989) Migration of fluid phases and genesis of basalt magmas in subduction zones. *J Geophys Res* 94:4697–4707
- Tatsumi Y, Eggins S (1995) *Subduction zone magmatism*. Blackwell Science, Boston
- Tomaru H, Ohsawa S, Amita K, Lu Z, Fehn U (2007) Influence of subduction zone settings on the origin of forearc fluids: Halogen concentrations and  $^{129}\text{I}/\text{I}$  ratios in waters from Kyushu, Japan. *Appl Geochem* 22:676–691
- Trommsdorff V, López Sánchez-Vizcaino V, Gomez-Pugnaire MT, Muntener O (1998) High pressure breakdown of antigorite to spinifex-textured olivine and orthopyroxene, SE Spain. *Contrib Mineral Petrol* 132:139–148
- Tropper P, Manning C (2004) Paragonite stability at 700 °C in the presence of H<sub>2</sub>O–NaCl fluids: constraints on H<sub>2</sub>O activity and implications for high pressure metamorphism. *Contrib Mineral Petrol* 147(6):740–749
- Ulmer P, Trommsdorff V (1995) Serpentine stability to mantle depths and subduction-related magmatism. *Science* 268:858–861
- Vanko DA (1986) High-chlorine amphiboles from oceanic rocks: product of highly-saline hydrothermal fluids? *Am Mineral* 71:51–59
- Vanko DA, Stakes DS (1991) Fluids in oceanic layer 3: evidence from veined rocks, Hole 735B, Southwest Indian Ridge. In: Von Herzen RP, Robinson PT, et al (eds) *Proceedings of the ocean*

- drilling program, Scientific results, vol 118. Ocean Drilling Program, College Station, TX, pp 181–215
- Volfinger M, Robert J-L, Vielzeuf D, Neiva AMR (1985) Structural control of the chlorine content of OH-bearing silicates (micas and amphiboles). *Geochim Cosmochim Acta* 49:37–48
- Wade JA, Plank T, Melson MG, Soto GJ, Hauri EH (2006) The volatile content of magmas from Arenal volcano, Costa Rica. *J Volcanol Geotherm Res* 157:94–120
- Wagner W, Pruß A (2002) The IAPWS formulation 1995 for the thermodynamic properties of ordinary water substance for general and scientific use. *J Phys Chem Ref Data* 31:387–535
- Wallace PJ (2005) Volatiles in subduction zone magmas: concentrations and fluxes based on melt inclusion and volcanic gas data. *J Volcanol Geotherm Res* 140:217–240
- Webster JD (2004) The exsolution of magmatic hydrosaline chloride liquids. *Chem Geol* 210:33–48
- Webster JD, Kinzler RJ, Mathez EA (1999) Chloride and water solubility in basalt and andesite melts and implications for magma degassing. *Geochim Cosmochim Acta* 63:729–738
- Wedepohl KH (1995) The composition of the continental crust. *Geochim Cosmochim Acta* 59:1217–1232
- Workman RK, Hart SR (2005) Major and trace element composition of the depleted MORB mantle (DMM). *Earth Planet Sci Lett* 231:53–72
- Workman RK, Hauri E, Hart SR, Wang J, Blusztajn J (2006) Volatile and trace elements in basaltic glasses from Samoa: implications for water distribution in the mantle. *Earth Planet Sci Lett* 241:932–951
- Wunder B, Schreyer W (1997) Antigorite: high-pressure stability in the system MgO-SiO<sub>2</sub>-H<sub>2</sub>O (MSH). *Lithos* 41:213–227
- Zimmer MM, Plank T, Hauri EH, Yogodzinski GM, Stelling P, Larsen J, Singer B, Jicha B, Mandeville C, Nye CJ (2010) The role of water in generating the calc-alkaline trend: new volatile data for Aleutian magmas and a new tholeiitic index. *J Petrol* 51:2411–2444